Electronic Supplementary Material (ESI) for Chemical Science.

Supporting Information for:

Proximal charge effects on guest binding to a non-polar pocket† ‡

Paolo Suating,[1] Thong T. Nguyen,[2] Nicholas E. Ernst,[1] Wang, Yang, [3] Jacobs H. Jordan,[4] Corinne L. D. Gibb,[1] Henry S. Ashbaugh,[3] and Bruce C. Gibb[1]*

[1] Department of Chemistry, Tulane University, New Orleans, LA 70118, USA

[2] Current address, Winder Laboratories, LLC, 716 Patrick Industrial Ln, Winder, GA 30680, USA

[3] Department of Chemical and Biomolecular Engineering, Tulane University, New Orleans, LA 70118, USA

[4] Current address, the Southern Regional Research Center Agricultural Research Service, USDA, 1100 Robert E. Lee Blvd, New Orleans, LA 70124, USA

† A contribution of reference data for the seventh statistical assessment of modelling of proteins and ligands (SAMPL7)

‡ Dedicated to Eric V Anslyn on the imminent arrival of his 60th birthday.

Table of Contents

Table of Figures

A. Hosts and guests used in this study

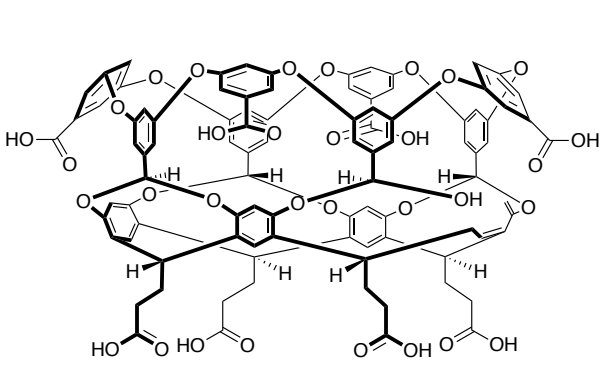

Octa-acid (**1**)

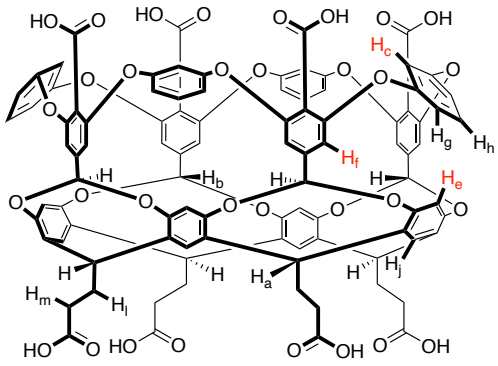

exo-Octa-acid (**2**)

Figure S1: Structures two hosts used in this study: octa-acid (**1**) and *exo*-octa-acid **(2**).

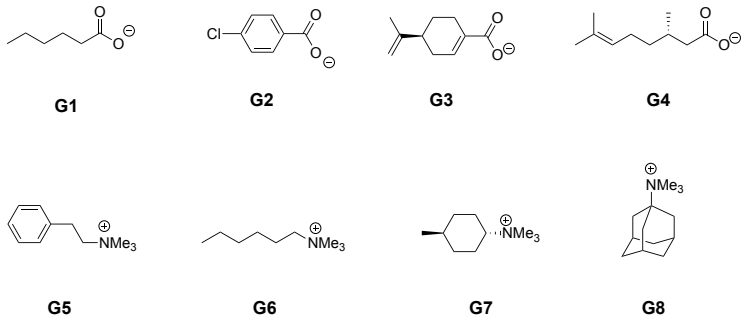

G1 **G2** **G3** **G4**

G5 **G6** **G7** **G8**

Figure S2: Guests used in this study. Guests **G5**–**G8** were used as their chloride salts.

B. Synthesis of host 2 *exo*-OA

All reagents were purchased from either Millipore Sigma, Fisher Scientific, or TCI America and were used without further purification unless otherwise specified. Solvents used in reactions were purchased from Millipore Sigma, and chromatography solvents were purchased from Fisher Scientific. All reactions involving anhyd solvents were performed under a blanket of dry N_2 gas. Resorcinol was recrystallised from boiling toluene and dried under high vacuum at rt overnight prior to use. *s*-Butyllithium was titrated against a 1.0 mM solution of diphenylacetic acid in anhydrous THF prior to use. TLC was performed using 60G F_{254} glass-backed silica gel plates from MilliporeSigma. All flash column chromatography separations were performed using a dry load on a Teledyne Isco CombiFlash NextGen300+ instrument using SiliCycle Silia*Sep* silica cartridges, or Teledyne Isco RediSep Rf Gold cartridges for compound **d**. All drying steps were performed under high vacuum. Degassing of solvents was performed by applying a vacuum on the solvent and replacing the atmosphere with N_2.

All ^{1}H NMR spectra and 2D NMR spectra were recorded on either a Bruker 500 MHz instrument or a Bruker Avance III 300 MHz instrument operating at 23 °C, using residual $CHCl_3$ (δ 7.26 ppm), DMSO-d_5 (δ 2.50 ppm), acetone-d_5 (δ 2.05 ppm), or H_2O (δ 4.79 ppm) as an internal standard. All ^{13}C NMR spectra were recorded on a Bruker Avance III 300 MHz instrument (75 MHz ^{13}C) operating at 23 °C using $CDCl_3$ (δ 77.16 ppm), acetone-d_6 (δ 29.84 ppm, 206.26 ppm), or DMSO-d_6 (δ 39.52 ppm) as an internal standard and are broadband decoupled. NMR spectra were processed using Mnova 11 (Mestrelab Research, S.L.). Multiplicity abbreviations are as follows: s – singlet; d – doublet; t – triplet; q – quartet; dd – doublet of doublets; dt – doublet of triplets; dq – doublet of quartets; td – triplet of doublets; tt – triplet of triplets; bs – broad singlet; m – unresolved multiplet. MALDI-MS spectra were collected on a Bruker Autoflex III MALDI/TOF mass spectrometer. ESI-MS spectra were collected on a Bruker micrOTOF ESI mass spectrometer.

Synthesis of copper(I) bromide–dimethyl sulfide complex

The purification[1] of copper(I) bromide and the synthesis of its dimethyl sulfide complex[2] used literature procedures. To a dry flask was added copper(I) bromide (50.0 g, 349 mmol) and glacial acetic acid (500 mL). The green suspension was stirred vigorously at rt under a blanket of N_2 for 24 h, filtered, the solids washed with absolute ethanol until the filtrate ran colourless, then dried under high vacuum at 110 °C for 24 h. The solids were transferred to a flame-dried, N_2-flushed flask and the solid contents cooled to –10 °C (1:1 ice/acetone). Dimethyl sulfide (300 mL) was then added dropwise via a pressure-equalising addition funnel over 30 min. and the suspension was allowed to stir at 0 °C for 30 mins. The resulting homogeneous, red-orange solution was heated to reflux (oil bath) for 24 h, after which time the solution was allowed to cool to rt. Hexanes (700 mL) was slowly poured onto the solution and the resulting suspension refrigerated for 4 h. The suspension was then filtered, and the solids washed with additional hexanes until the filtrate ran colourless. The solids were dried under high vacuum at rt overnight to afford the complex as a greyish-white crystalline powder (70.5 g, 98%). The complex was stored in a desiccator until ready for use. Crystallographic data agree with the literature.[2]

Synthesis of propanol-footed meta-basket b

To a flame-dried, N_2-flushed flask was sequentially added octabromide **a** (7.34 g, 4.31 mmol), pyridine (200 mL), resorcinol (2.85 g, 25.8 mmol, 6.0 equiv.), and potassium carbonate (7.14 g, 51.7 mmol, 12 equiv.). At each of these additions, the resulting suspension was sparged with N_2 for 10 minutes to exclude dissolved and atmospheric oxygen. Copper(I) bromide–dimethyl sulfide (10.6 g, 51.7 mmol, 12 equiv.) was then added in one portion, and the suspension was heated to vigorous reflux (sand bath) for 10 d. The solvent was removed, and the residue dried under high vacuum at rt for 2 h. The solids were taken up in 250 mL THF, sonicated for 30 mins, then filtered through a THF-wet Celite pad. The Celite was washed with additional THF until the

filtrate ran colourless. The solvent was removed from the combined filtrate under reduced pressure, and the residue dried under high vacuum at rt overnight. This residue was then taken up in 3 M aqueous HCl, sonicated for 45 minutes, filtered, washed with dH_2O until the filtrate was neutral, and dried under high vacuum at 110 °C for 6 h. The solids were taken up in 50 mL hexanes/ethyl acetate (1:1), sonicated for 5 mins, filtered, and washed with additional hexanes/ethyl acetate until the filtrate ran colourless. The solids were dried under high vacuum at 110 °C overnight to afford crude propanol-footed meta-basket **b** (5.43 g, 84% crude) as a tan solid.

TIPS-footed meta-basket c

To a flame-dried, N_2-flushed flask containing anhydrous THF (200 mL) was added crude propanol-footed meta-basket **b** (5.43 g, 3.63 mmol) and imidazole (2.17 g, 31.9 mmol, 8.8 equiv.). To the resulting dark-coloured mixture was added *N*,*N*-diisopropylethylamine (5.6 mL, 31.9 mmol, 8.8 equiv.) and chloro(triisopropyl)silane (6.8 mL, 31.9 mmol, 8.8 equiv.). This mixture was heated to reflux (oil bath) for 48 h, after which time the solvent was removed under reduced pressure and the residue dried under high vacuum at rt overnight. The crude product was then subjected to flash column chromatography using a gradient of 0–5% EtOAc in hexanes (R_f = 0.36, 5% EtOAc in hexanes). After removal of the mobile phase under reduced pressure the resulting solid was suspended in 25 mL hexanes and sonicated for 3 min, refrigerated, and filtered to give the product **c** as a white powder which was dried under high vacuum at 110 °C overnight (1.96 g, 50%). ^{1}H NMR (500 MHz, $CDCl_3$) δ 1.06 (m, 84H), 1.55 (tt, *J* = 7.4, 6.4 8H), 2.27 (td, *J* = 8.1, 7.4 Hz, 8H), 3.75 (t, *J* = 6.4 Hz, 8H), 4.5 (s, 4H), 4.75 (t, *J* = 8.4 Hz, 4H), 5.95 (s, 4H), 6.50 (d, *J* = 2.4 Hz, 8H), 6.62 (t, *J* = 2.4 Hz, 4H), 6.97 (t, *J* = 2.4 Hz, 4H), 7.15 (s, 4H), 7.21 (dd, *J* = 8.2, 2.4 Hz, 8H), 7.55 (t, *J* = 8.2 Hz, 4H). ^{13}C{^{1}H} NMR (75 MHz, $CDCl_3$) δ 12.2, 18.2, 26.7, 31.2, 36.3, 63.0, 105.8, 107.7, 109.8, 115.2, 115.9, 120.7, 122.4, 131.4, 137.0, 139.4, 156.5, 156.7, 161.3. HRMS (MALDI/TOF) m/z: $[M + Na]^+$ Calcd. for $C_{128}H_{152}O_{20}Si_4Na$ 2144.98; Found 2144.95. Anal. Calcd. for $C_{128}H_{152}O_{20}Si_4 \cdot 2H_2O$: C, 71.21; H, 7.28. Found: C, 70.98; H, 6.90.

Synthesis of tetra-*exo*-ester TIPS-meta-basket d

To a flame-dried, N_2-flushed flask was added TIPS-meta-basket **c** (1.20 g, 0.57 mmol) and anhydrous THF (100 mL). The resulting solution was cooled to –78 °C (acetone/CO_2) for 30 mins, before *sec*-butyllithium (1.05 M in cyclohexane, 5.5 mL, 5.8 mmol, 10.2 equiv.) was added dropwise via syringe over 30 mins. The yellow solution was then left to stir for an additional 30 mins at –78 °C, after which ethyl chloroformate (0.6 mL in 5 mL anhydrous THF, 6.2 mmol, 11 equiv.) was added via syringe dropwise over 30 mins. The solution was left to stir for 1 h, after which the yellow solution was allowed to warm to rt and stirred for a total of 1 h. Aqueous HCl (1 M, 2.5 mL) was added slowly to quench the solution, the solvent was removed under reduced pressure, and the resulting solid foam residue dried under high vacuum at rt for 30 mins. The residue was taken up in 50 mL $CHCl_3$ and was washed with 3 × 20 mL dH_2O, and 1 × 20 mL saturated aqueous NaCl. The organic layer was dried with anhydrous Na_2SO_4, filtered, and the solvent removed under reduced pressure. The residue was then dried under high vacuum at 110 °C overnight and the crude solids were subjected to flash column chromatography using 99:1 $CHCl_3$/EtOAc with a flow rate of 25 mL/min (R_f = 0.22, 2% EtOAc in hexanes). This afforded the product as a white solid which was dried under high vacuum at 110 °C overnight (0.58 g, 44%). ^{1}H NMR (500 MHz, $CDCl_3$) δ 1.06 (m, 84H), 1.39 (t, *J* = 7 Hz, 12H), 1.54 (m, 8H), 2.26 (q, *J* = 7 Hz, 8H), 3.74 (t, *J* = 6 Hz, 4H), 4.45 (q, *J* = 7 Hz, 8H), 4.48 (s, 4H), 4.73 (t, *J* = 8 Hz, 4H), 5.87 (s 4H), 6.53 (d, *J* = 1 Hz, 8H), 6.72 (t, *J* = 2 Hz, 4H), 7.15 (s, 4H), 7.24 (dd, *J* = 2, 8 Hz, 8H), 7.56 (t, *J* = 8 Hz, 4H). ^{13}C{^{1}H} NMR (75 MHz, $CDCl_3$) δ 12.2, 14.4, 18.2, 26.7, 31.1, 36.3, 62.0, 62.9, 106.0, 109.4, 115.1, 115.9, 121.0 122.5, 131.3, 137.0, 140.2, 156.3, 156.4, 158.0, 164.8. HRMS (MALDI/TOF) m/z: $[M + Na]^+$ Calcd. for $C_{140}H_{168}O_{28}Si_4Na$ 2432.07; Found 2432.56. Anal. Calcd. for $C_{140}H_{168}O_{28}Si_4$: C, 69.74; H, 7.02. Found: C, 69.45; H, 7.15.

Synthesis of tetra-*exo*-ester tetrol meta-basket e

To a dry flask was added tetra-*exo*-ester TIPS-meta-basket **d** (0.28 g, 0.12 mmol) and THF (25 mL). The mixture was stirred until homogeneous, and to which was then added TBAF·3H_2O (0.22 g, 0.70 mmol, 6 equiv.). The resulting solution was allowed to stir at rt overnight, after which the solvent was removed under reduced pressure, and the residue dried under high vacuum at rt for 1 h. The residue was taken up in 20 mL $CHCl_3$ and was washed with 3 × 20 mL dH_2O and 1 × 20 mL saturated aqueous NaCl. The organic layer was dried with anhydrous Na_2SO_4, filtered, the solvent removed under reduced pressure, and the residue dried under high vacuum at rt for 2 h. The residue was taken up in 10 mL diethyl ether, sonicated for 3 mins, refrigerated for 2 h, filtered, washed with additional cold diethyl ether, and dried under high vacuum under high vacuum at 110 °C overnight to afford tetra-*exo*-ester tetrol meta-basket **e** as a white powder (0.16 g, 77%). ^{1}H NMR (300 MHz, DMSO-d_6) δ 1.27 (t, *J* = 7 Hz, 12H), 1.40 (m, 8H), 2.39 (m, 8H), 3.47 (q, *J* = 5.8 Hz, 8H), 4.37 (q, *J* = 7 Hz, 8H), 4.40 (s, 4H), 4.49 (t, *J* = 4.8 Hz, 4H), 4.54 (t, *J* = 8.3 Hz, 4H), 5.74 (s, 4H), 6.46 (s, 8H), 6.65 (t, *J* = 1.7 Hz, 8H), 7.40 (dd, *J* = 1.9, 6.2 Hz), 7.74 (m, 12H). ^{13}C{^{1}H} NMR (75 MHz, DMSO-d_6) δ 14.0, 26.0, 30.5, 36.2, 105.7, 108.6, 113.7, 114.5, 114.6, 120.6, 125.2, 132.0, 136.7, 139.6, 155.1, 155.6, 156.9, 163.6. HRMS (MALDI/TOF) m/z: [M + Na]$^+$ Calcd. for $C_{104}H_{88}O_{28}Na$ 1807.53; Found 1807.52. Anal. Calcd. for $C_{104}H_{88}O_{28}·CHCl_3·Et_2O$: C, 66.14; H, 5.04. Found: C, 66.10; H, 5.01.

Synthesis of tetra-*exo*-ester tetra-acid f

To a flame-dried, N_2-flushed flask was added tetra-*exo*-ester tetrol meta-basket **e** (0.160 g, 0.09 mmol), DMA (10.0 mL), and anhydrous *t*-BuOH (10.0 mL). The solution was then stirred until homogeneous, at which point $KMnO_4$ (0.198 g, 1.25 mmol, 14 equiv.) was added. The solution was allowed to stir at rt for 48 h, after which time the resulting suspension was filtered, and the residue taken up in 50 mL 1:1 DMA/H_2O, sonicated, filtered, and washed with 20 mL dH_2O. The solvent from the combined filtrates was removed under reduced pressure and the resulting residue dried under high vacuum at rt for 4 h. The resulting solid was then added to 10 mL conc. HCl. The suspension was sonicated for 5 mins, diluted with 20 mL dH_2O, filtered, and the solids washed with additional dH_2O until the filtrate was neutral. The solids were dried under high vacuum at 110 °C overnight to afford tetra-*exo*-ester tetra-acid (0.141 g, 87%) as an off-white powder. ^{1}H NMR (300 MHz, DMSO-d_6) δ 1.28 (t, *J* = 7 Hz, 12H), 2.22 (q, *J* = 2 Hz, 8H), 2.62 (q, *J* = 2 Hz, 8H), 4.38 (q, *J* = 7 Hz, 8H), 4.40 (s, 4H), 4.60 (t, *J* = 8 Hz, 4H), 5.75 (s, 4H), 6.47 (s, 8H), 6.65 (t, *J* = 2 Hz, 4H), 7.40 (dd, *J* = 2, 8 Hz, 8H), 7.74 (m, 8H), 12.17 (s, 4H). ^{13}C{^{1}H} NMR (75 MHz, DMSO-d_6) δ 14.5, 25.5, 32.3, 36.3, 62.0, 106.4, 109.1, 114.6, 115.1, 115.3, 121.2, 125.3, 132.6, 136.7, 140.1, 155.9, 156.2, 157.5, 164.1, 174.3. HRMS (MALDI/TOF) m/z: [M + Na]$^+$ Calcd for $C_{104}H_{80}O_{32}Na$ 1863.45; Found 1863.46. Anal. Calcd for $C_{104}H_{80}O_{32}·4H_2O$: C, 65.27; H, 4.63. Found: C, 65.59; H, 4.67.

Synthesis of *exo*-Octa Acid 2

To a round bottomed flask was added tetra-*exo*-ester tetra acid (0.176 g, 0.096 mmol), pyridine (20 mL) and 2 M aqueous LiOH (1.43 mL, 2.9 mmol, 30 equiv.). The suspension was stirred at reflux (oil) for 48 h, during which time dH_2O was added dropwise to dissolve any precipitate formed. After this time the homogeneous solution was allowed to cool to rt, and the solvent removed under reduced pressure. The residue was dried at rt for 2 h after which conc. HCl (10 mL) was added and the suspension sonicated for 5 mins. The suspension was diluted with dH_2O (20 mL), filtered, and the solids washed with additional dH_2O until the filtrate was neutral. The residue was dried under high vacuum at rt for 4 h, after which it was dissolved in minimum acetone, triturated with 20 volumes of dH_2O, refrigerated for 1 h, and filtered. The residue was dried under high vacuum at 110 °C for 24 h to afford *exo*-octa acid **2** (0.130 g, 79%) as an off-white powder. ^{1}H NMR (300 MHz, DMSO-d_6) δ 2.21 (m, 8H), 2.62 (m, 8H), 4.40 (s, 4H),

4.60 (t, *J* = 13.5 Hz, 4H), 5.76 (s, 4H), 6.45 (s, 8H), 6.68 (t, *J* = 3.5 Hz, 4H), 7.36 (dd, *J* = 3.4, 13.2 Hz, 8H), 7.72 (m, 12H). ^{1}H NMR (500 MHz, D_2O) δ 2.22 (t, *J* = 7.25 Hz, 8H), 2.60 (q, *J* = 7.5 Hz, 8H), 4.52 (s, 4H), 4.63 (t, *J* = 8.15, 4H), 5.95 (s, 4H), 6.51 (s, 8H), 6.93 (t, *J* = 2.3 Hz, 4H), 7.34 (dd, *J* = 2.3, 8.2 Hz, 8H), 7.51 (s, 4H), 7.67 (t, *J* = 8.2 Hz, 8H). ^{13}C{^{1}H} NMR (75 MHz, DMSO-d_6) δ 25.1, 31.9, 35.9, 105.9, 108.9, 114.2, 115.0, 116.5, 120.6, 124.9, 132.0, 136.2, 138.9, 155.5, 155.9, 156.6, 165.0, 173.9. HRMS (ESI) m/z: $[M - 4H^+]^{4-}$ Calcd for $C_{96}H_{64}O_{32}$ 431.3281; Found 431.3261.

Optional purification of propanol-footed meta-basket b via the tetra-acetate b'

To a flame-dried, N_2-flushed flask was added crude **b** (0.109 g, 0.07 mmol) and acetic anhydride (10 mL). The suspension was stirred at 100 °C (oil bath) for 18 hours, after which the homogeneous solution was cooled to rt, and the solvent removed under reduced pressure. The dark brown residue was then dried under high vacuum at 110 °C for 4 h. After this time the residue were subjected to flash column chromatography (100% $CHCl_3$, ethanol preservative, R_f = 0.10, $CHCl_3$ with ethanol preservative). Combining the resulting fractions containing the product, removal of the solvent under reduced pressure, and dying under high vacuum at 110 °C yielded **b'** as an off-white solid (0.076 g, 63%). The solids were then dissolved in DMA (5 mL), and to the resulting solution was added 1 M aqueous LiOH (0.70 mL, 16 equiv.) dropwise. The suspension was then stirred at 60 °C for 72 h, after which the solvent was removed from the homogeneous mixture under reduced pressure and the residue dried under high vacuum at rt for 3 h. The solids were then suspended in 1 M aqueous HCl (10 mL) and sonicated for 10 mins. The suspension was filtered, and the solids were dried under high vacuum at 110 °C for 1 h. The solids were then taken up in 1:1 hexanes/$CHCl_3$ (10 ml), sonicated for 5 mins, and the suspension filtered. The solids were then dried under high vacuum at 110 °C overnight to afford pure **b** as a white powder (0.03 g, 44%). ^{1}H NMR (400 MHz, $CDCl_3$) δ 1.64 (dq, *J* = 13.4, 6.3 Hz, 8H), 2.04 (s, 12H), 2.28 (q, *J* = 8.0 Hz, 8H), 4.12 (t, *J* = 6.5 Hz, 8H), 4.49 (s, 4H), 4.78 (t, *J* = 8.2 Hz, 4H), 5.95 (s, 4H), 6.46 (d, *J* = 2.3 Hz, 8H), 6.60 (t, *J* = 2.2 Hz, 4H), 6.96 (d, *J* = 2.4 Hz, 4H), 7.10 (s, 4H), 7.20 (dd, *J* = 8.1, 2.2 Hz, 8H), 7.55 (t, *J* = 8.1 Hz, 4H). ^{13}C{^{1}H} NMR (75 MHz, $CDCl_3$) δ 20.95, 26.85, 36.01, 63.85, 105.53, 107.62, 109.64, 115.37, 115.65, 120.60, 121.82, 131.17, 136.50, 138.98, 156.48, 156.55, 161.17, 171.00. HRMS (MALDI/TOF) m/z: $[M + Ag]^+$ Calcd. for $C_{100}H_{80}O_{24}Ag$ 1771.41; Found 1771.81. Anal. Calcd. for $C_{100}H_{80}O_{24}\cdot H_2O$: C, 71.34; H, 4.91. Found: C, 71.66, H, 5.21.

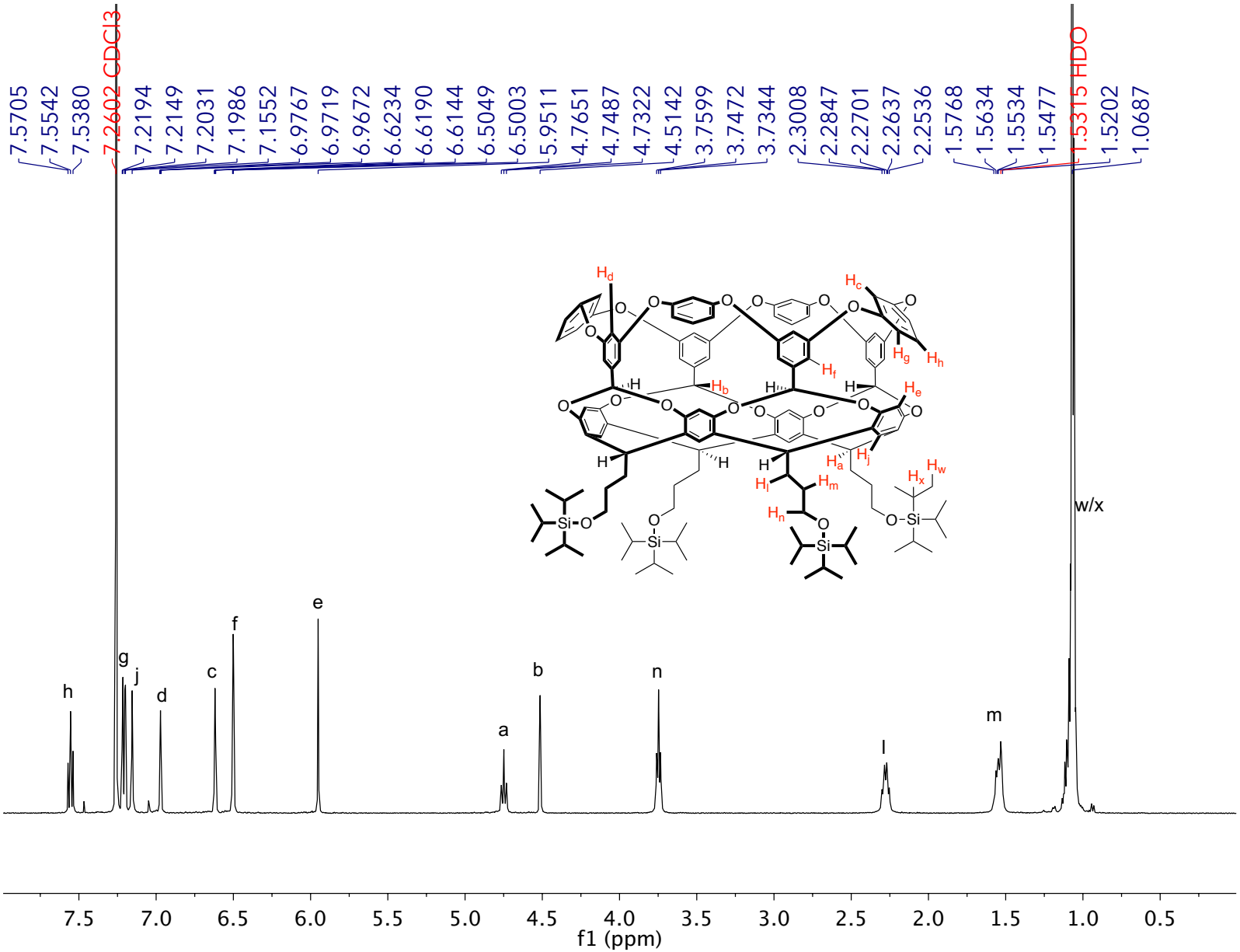

Figure S3: ^{1}H NMR spectrum of TIPS-footed meta-basket **c** in $CDCl_3$.

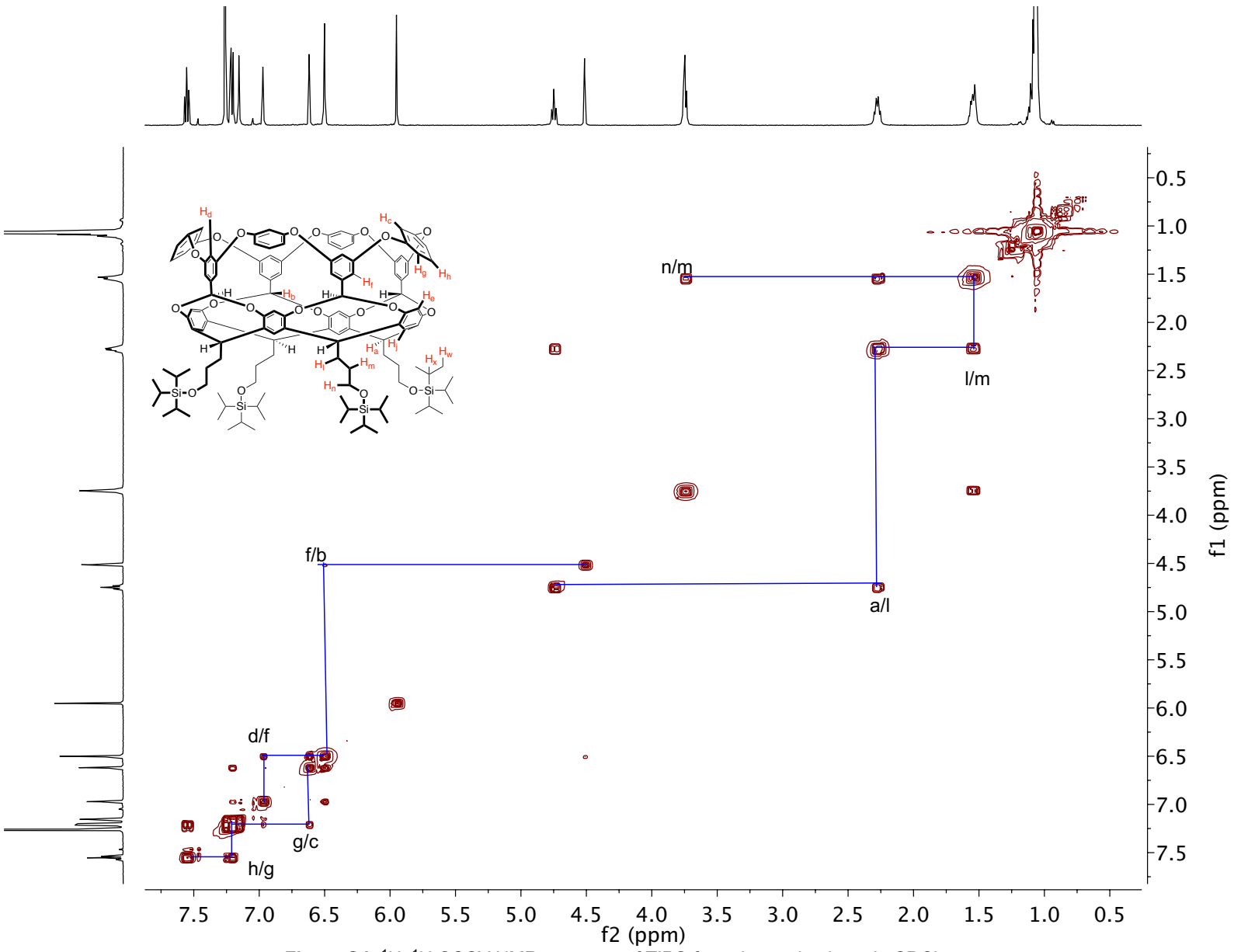

Figure S4: ^{1}H–^{1}H COSY NMR spectrum of TIPS-footed meta-basket **c** in $CDCl_3$.

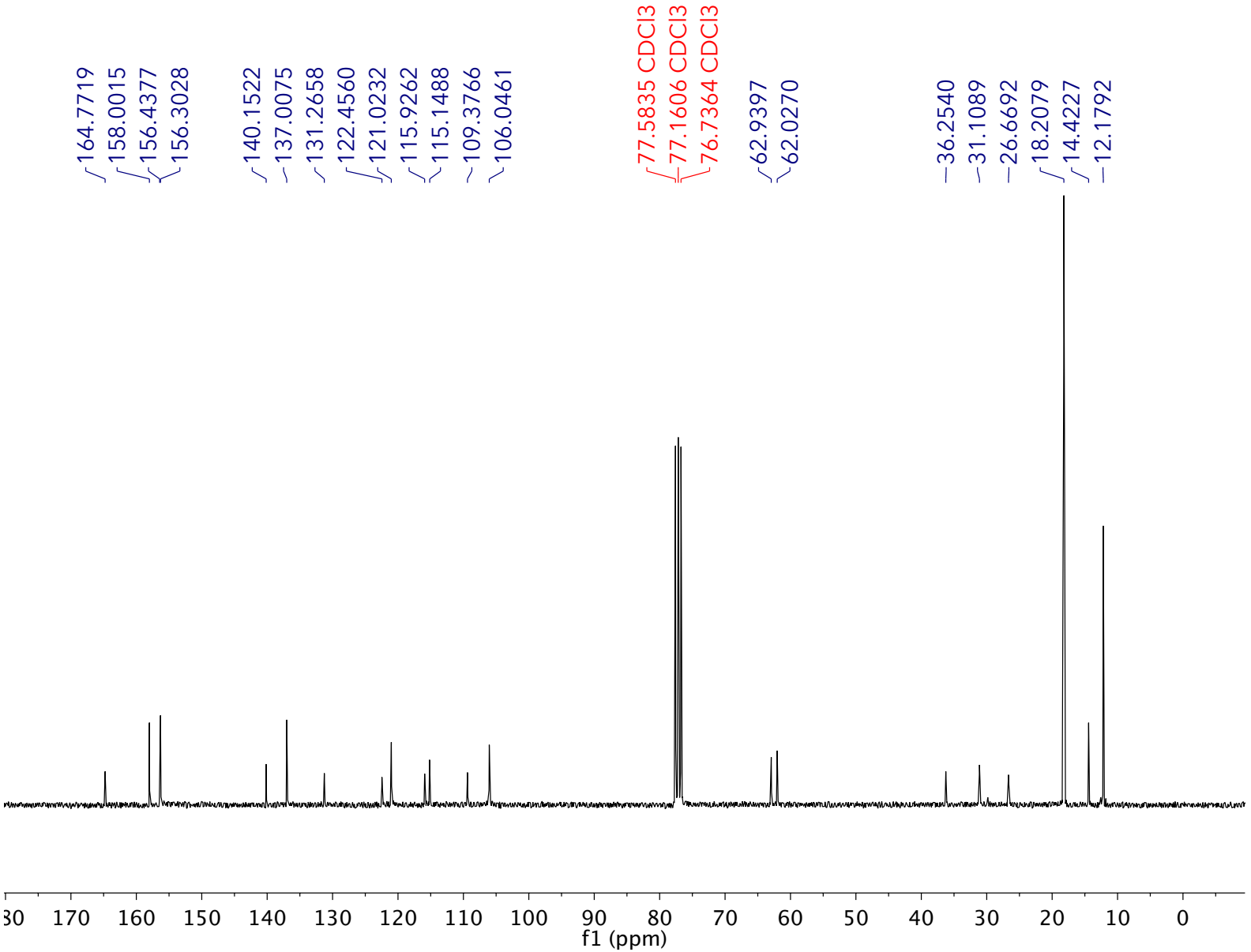

Figure S5: ^{13}C NMR spectrum of TIPS-footed meta-basket **c** in $CDCl_3$.

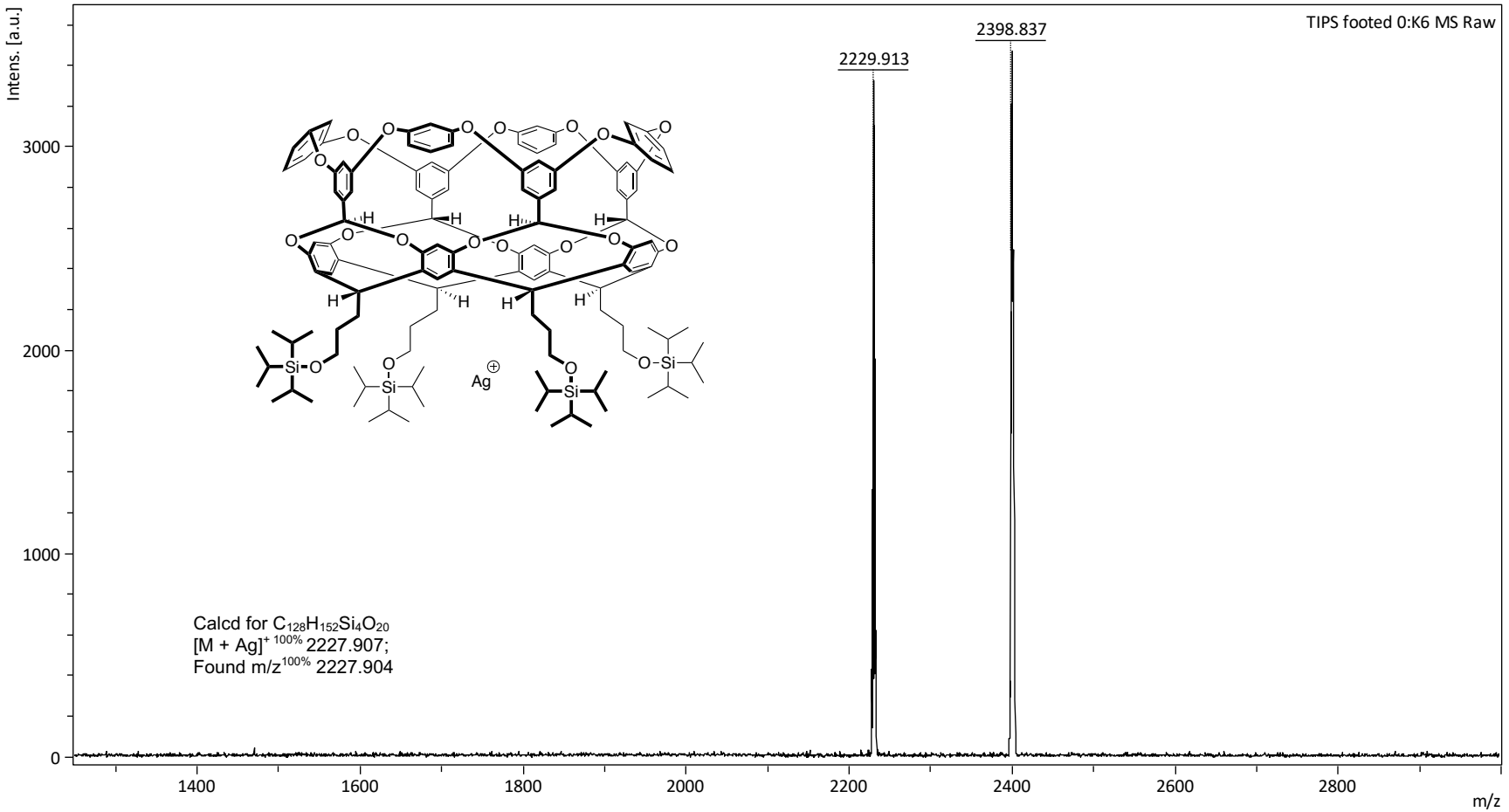

Figure S6: MALDI-MS of TIPS-footed meta-basket **c** (2:1:1 analyte/DCTB/$AgNO_3$), 2 mg ml^{-1} in $CHCl_3$. $[M + Ag]^+$ is indicated by signal at m/z 2229.913; $[M + Ag + AgNO_3]^+$ is indicated by signal at m/z 2398.837.

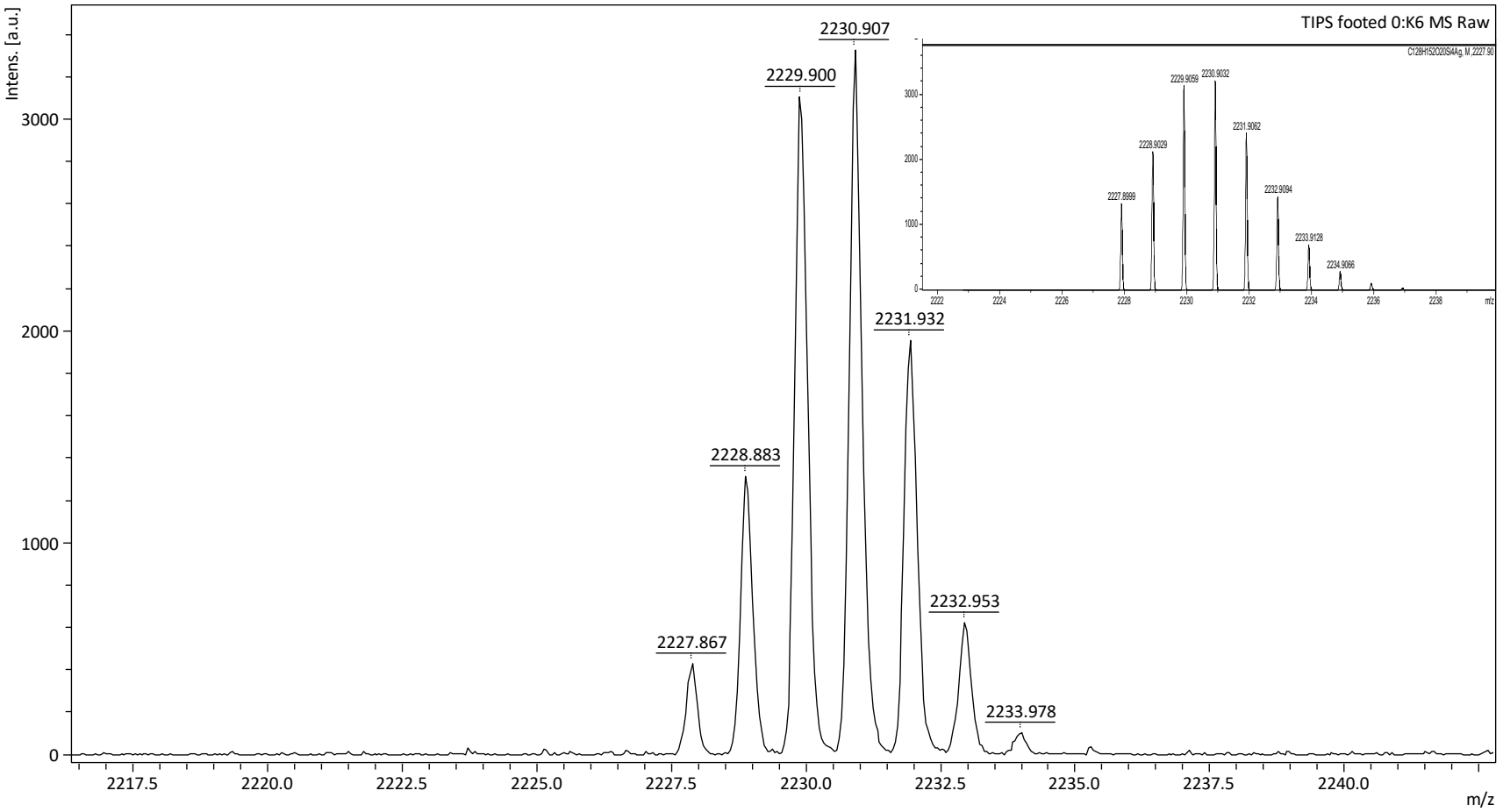

Figure S7: Expanded view of TIPS-meta-basket **b** $[M + Ag]^+$ with theoretical calculation inset.

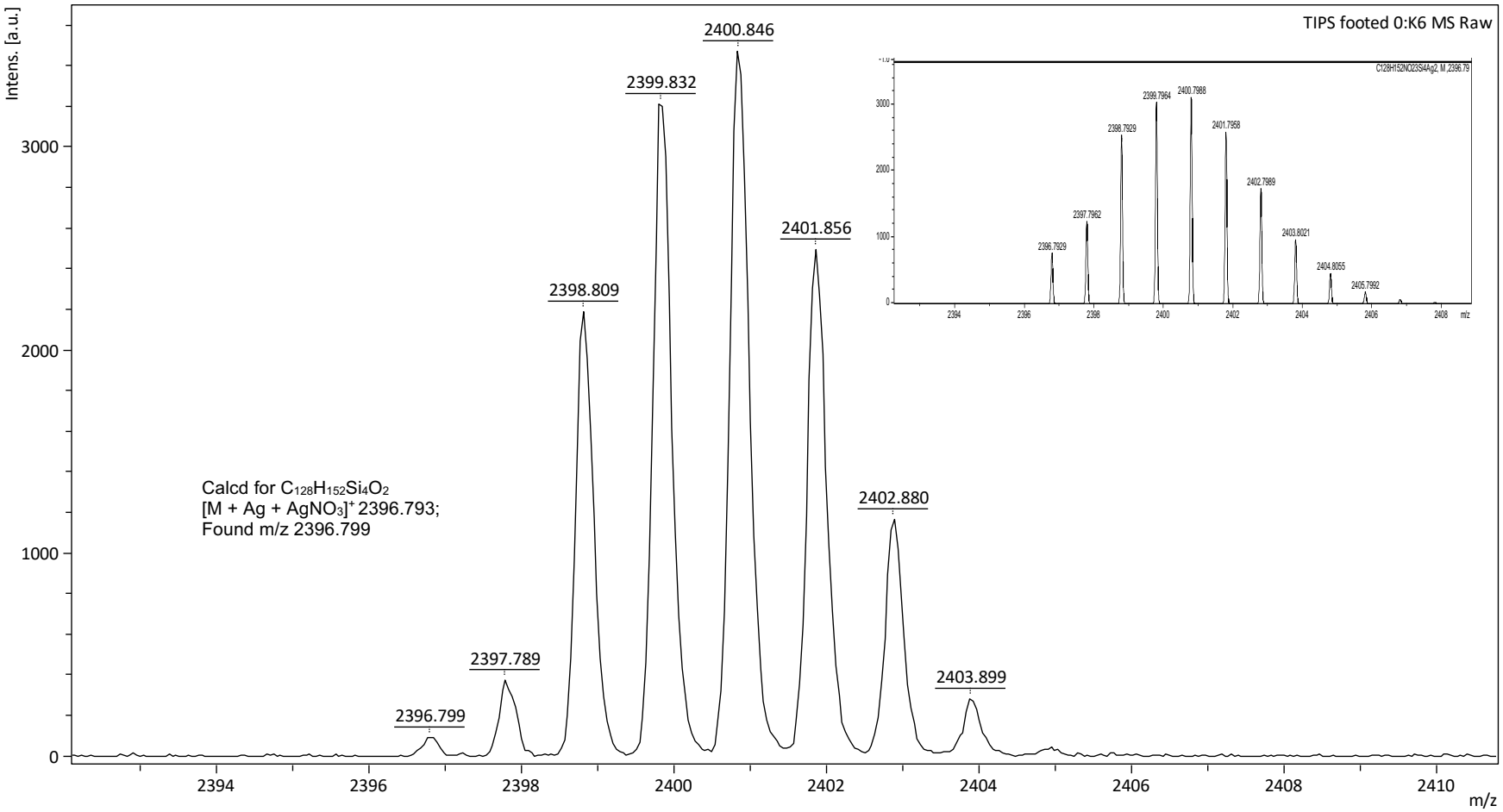

Figure S8: Expanded view of TIPS-meta-basket **b** $[M + Ag + AgNO_3]^+$ with theoretical calculation inset.

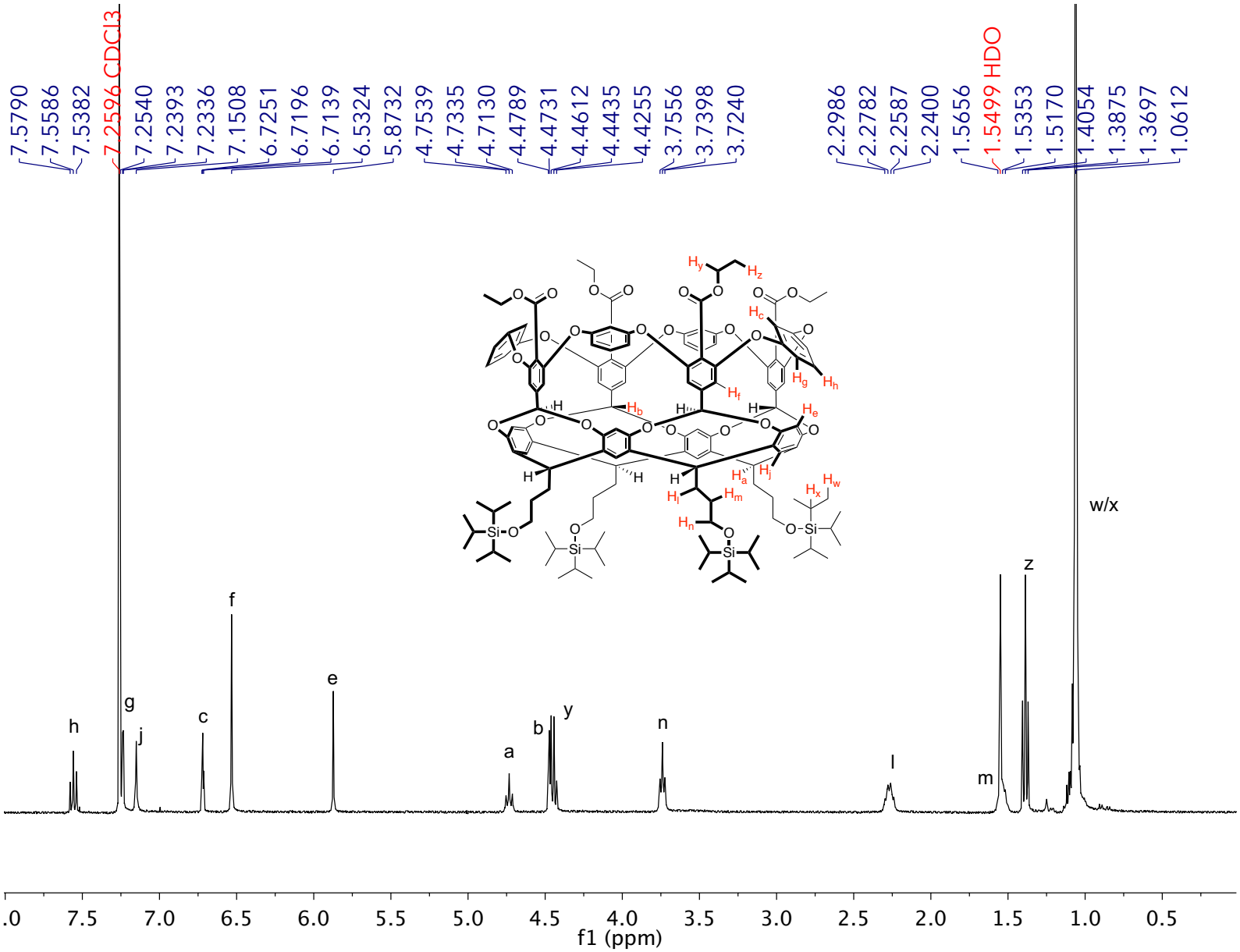

Figure S9: ^{1}H NMR spectrum of tetra-*exo*-ester TIPS-meta-basket **d** in $CDCl_3$.

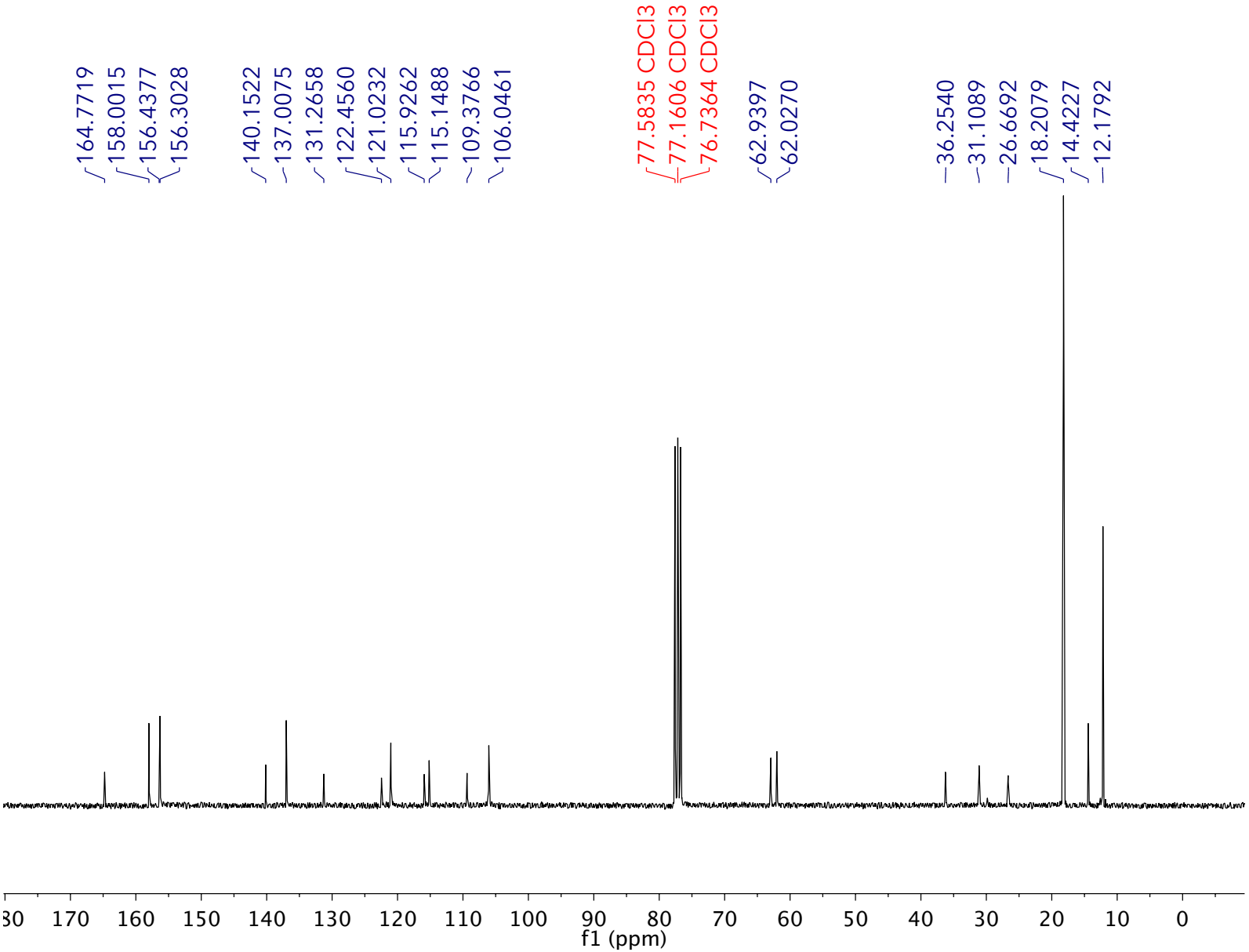

Figure S10: ^{13}C NMR spectrum of tetra-*exo*-ester TIPS-meta-basket **d** in $CDCl_3$.

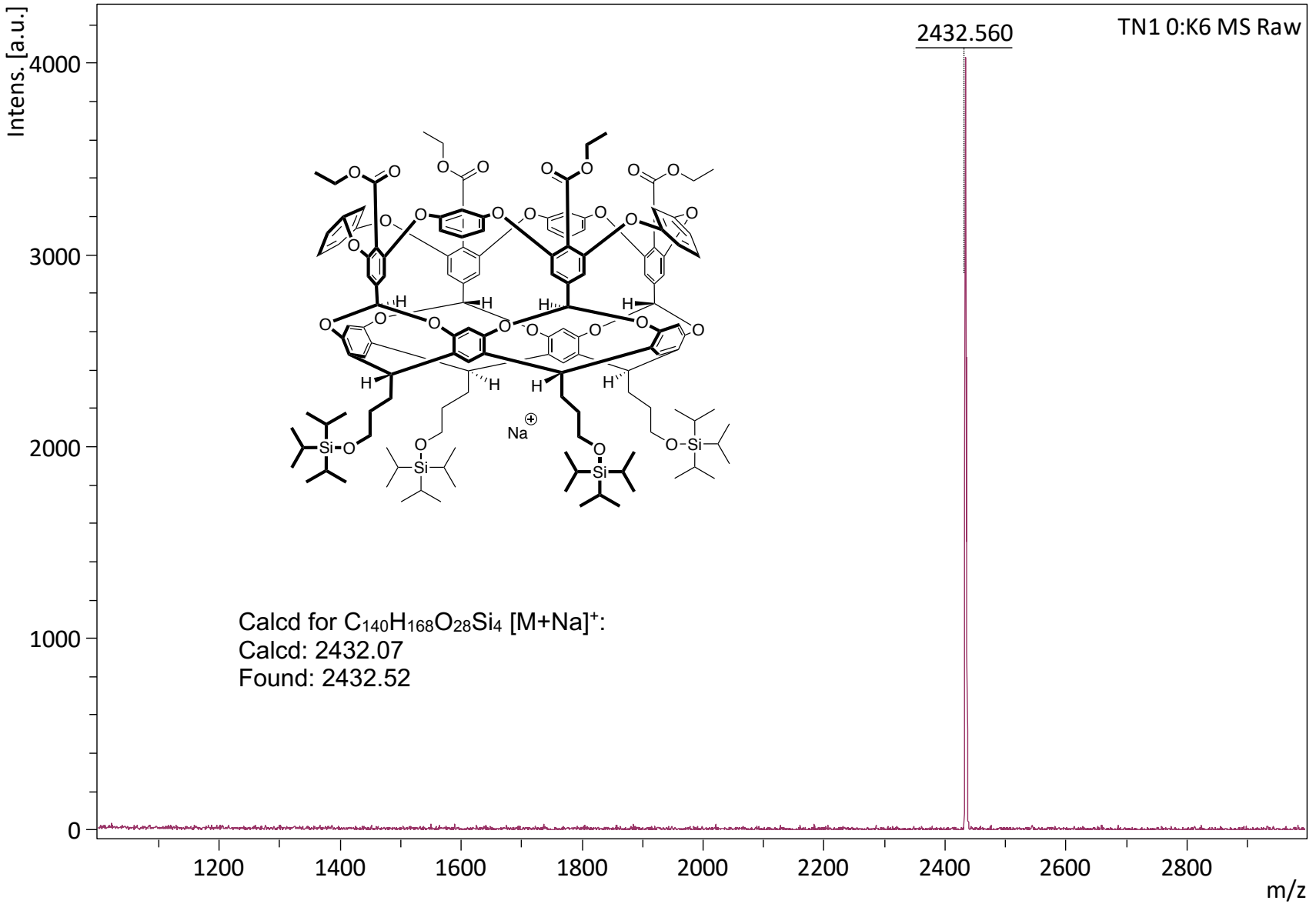

Figure S11: MALDI-TOF MS of tetra-*exo*-TIPS meta-basket **d** $[M + Na]^+$ (2:1:1 2 mg ml^{-1} in $CHCl_3$/DCTB/NaTFA).

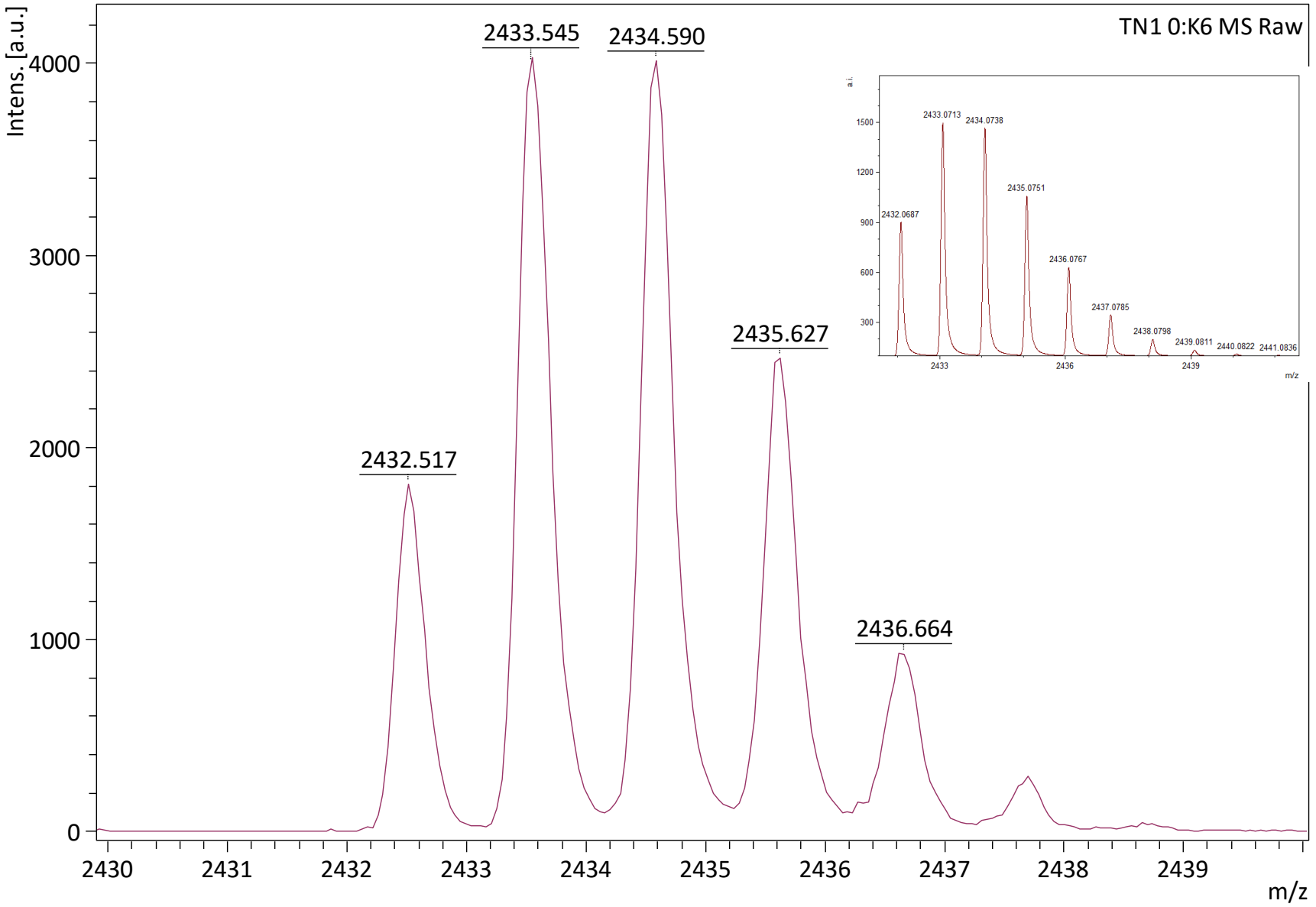

Figure S12: Expanded view of tetra-*exo*-ester TIPS meta-basket **d** $[M + Na]^+$ with theoretical calculation inset.

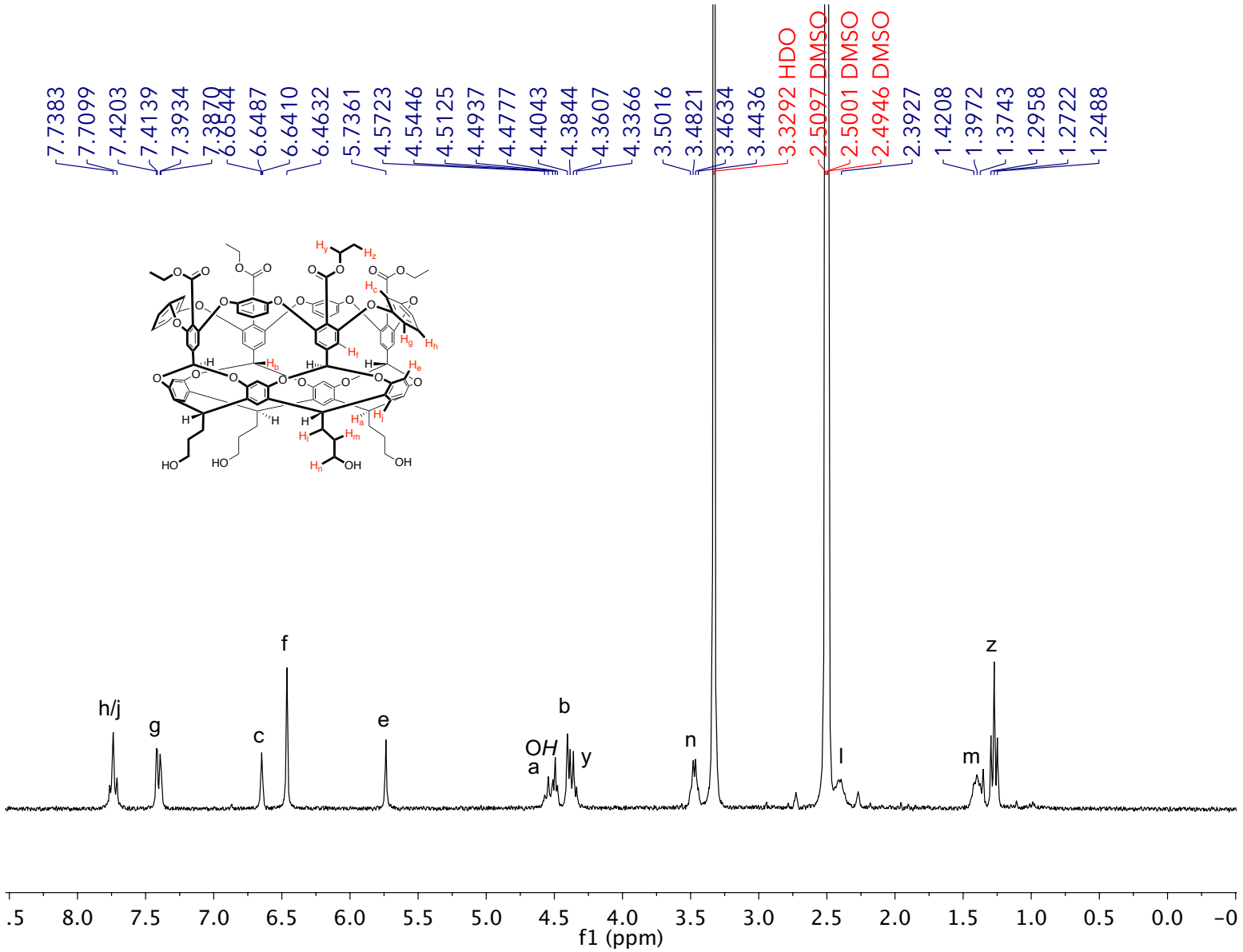

Figure S13: ^{1}H NMR spectrum of tetra-*exo*-ester tetrol meta-basket **e** in DMSO-d_6.

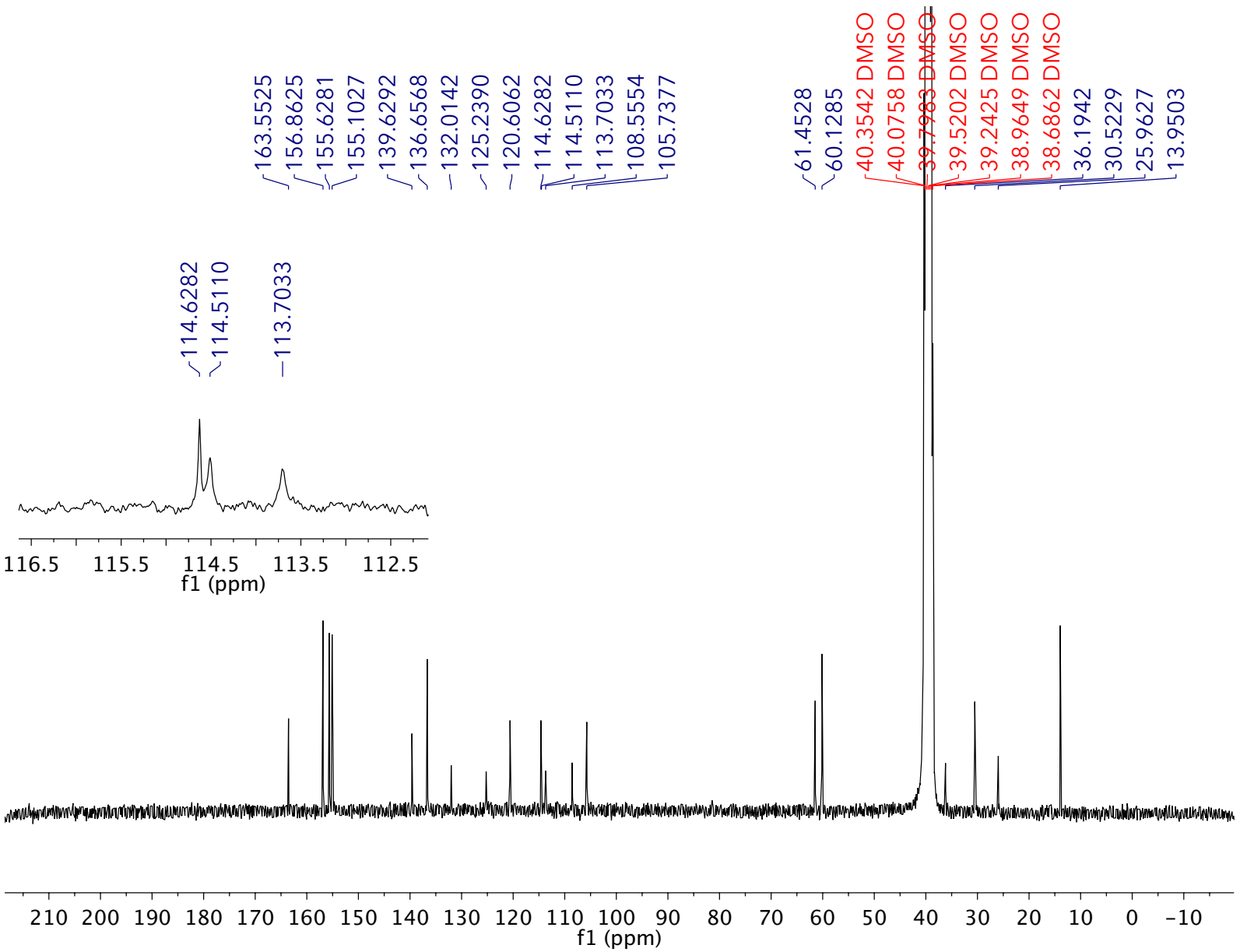

Figure S14: ^{13}C NMR spectrum of tetra-*exo*-ester tetrol meta-basket **e** in DMSO d-$_6$. Inset shows expanded region from 112.5 ppm to 116.5 ppm.

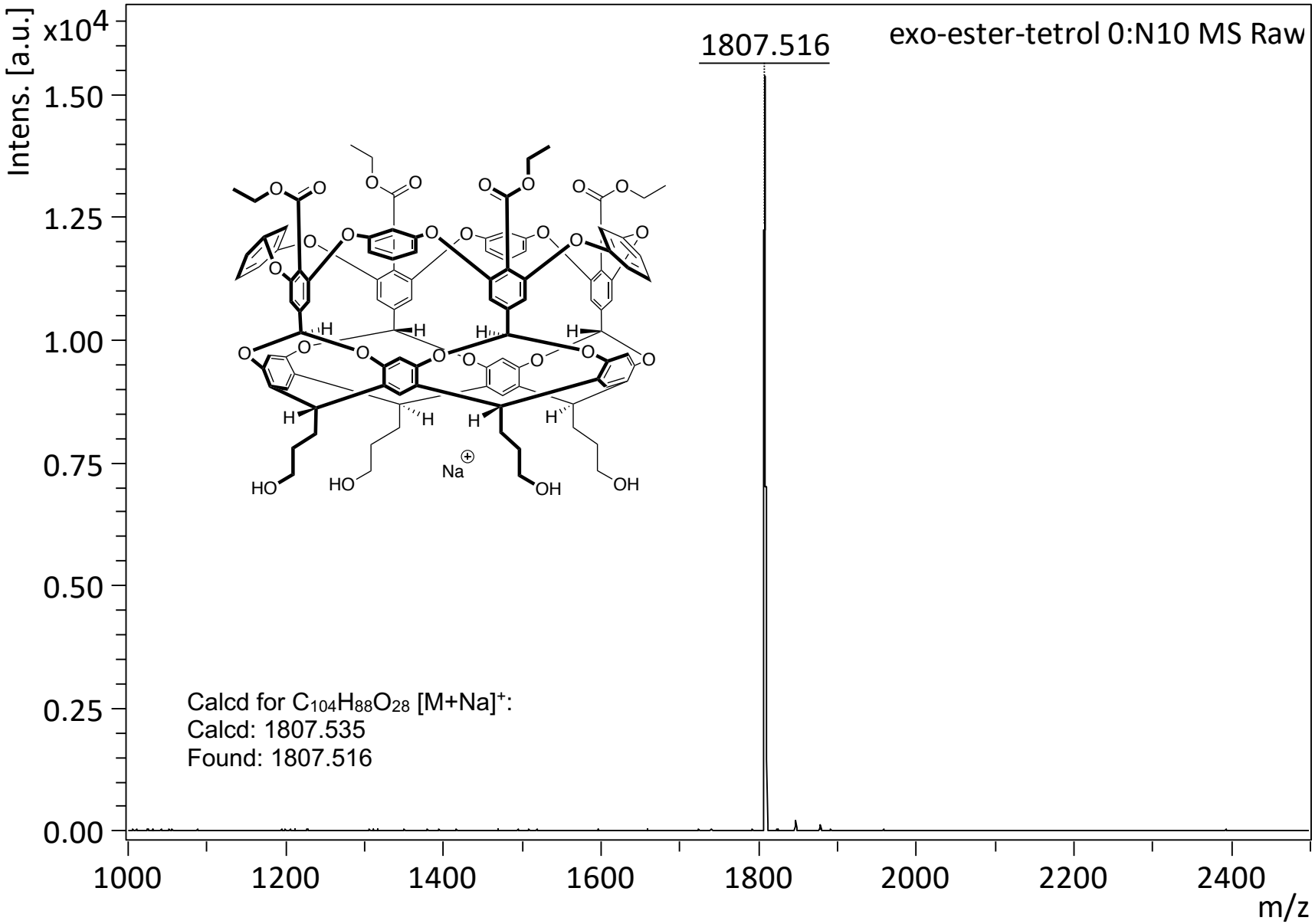

Figure S15: MALDI-TOF MS of tetra-*exo*-ester tetrol meta-basket **e** $[M + Na]^+$ (2:1:1 2 mg ml^{-1} in THF/CHCA/NaTFA).

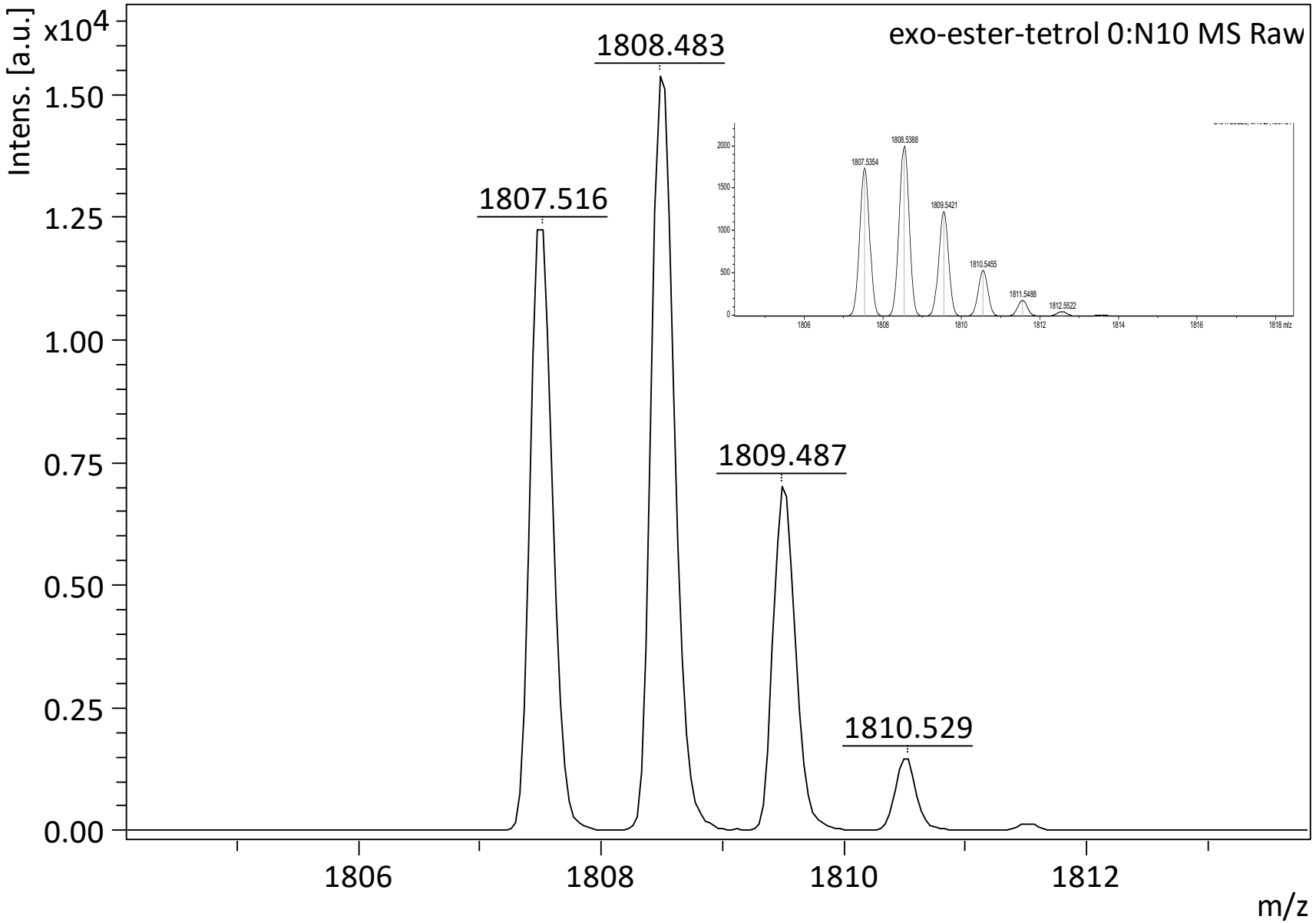

Figure S16: Expanded view of tetra-*exo*-ester tetrol meta-basket **e** with theoretical calculation inset.

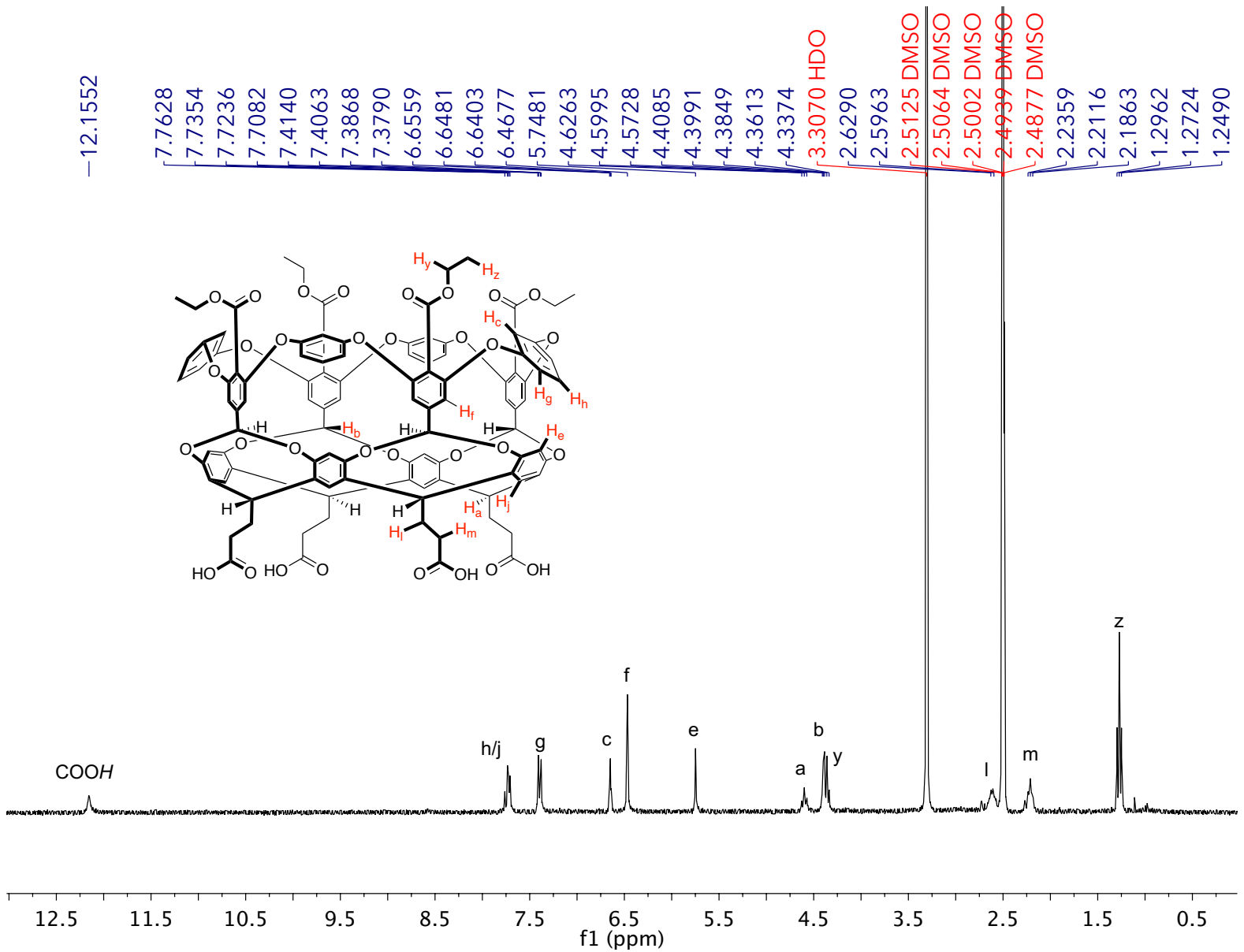

Figure S17: ^{1}H NMR of tetra-*exo*-ester tetra-acid **f** in DMSO-d_6.

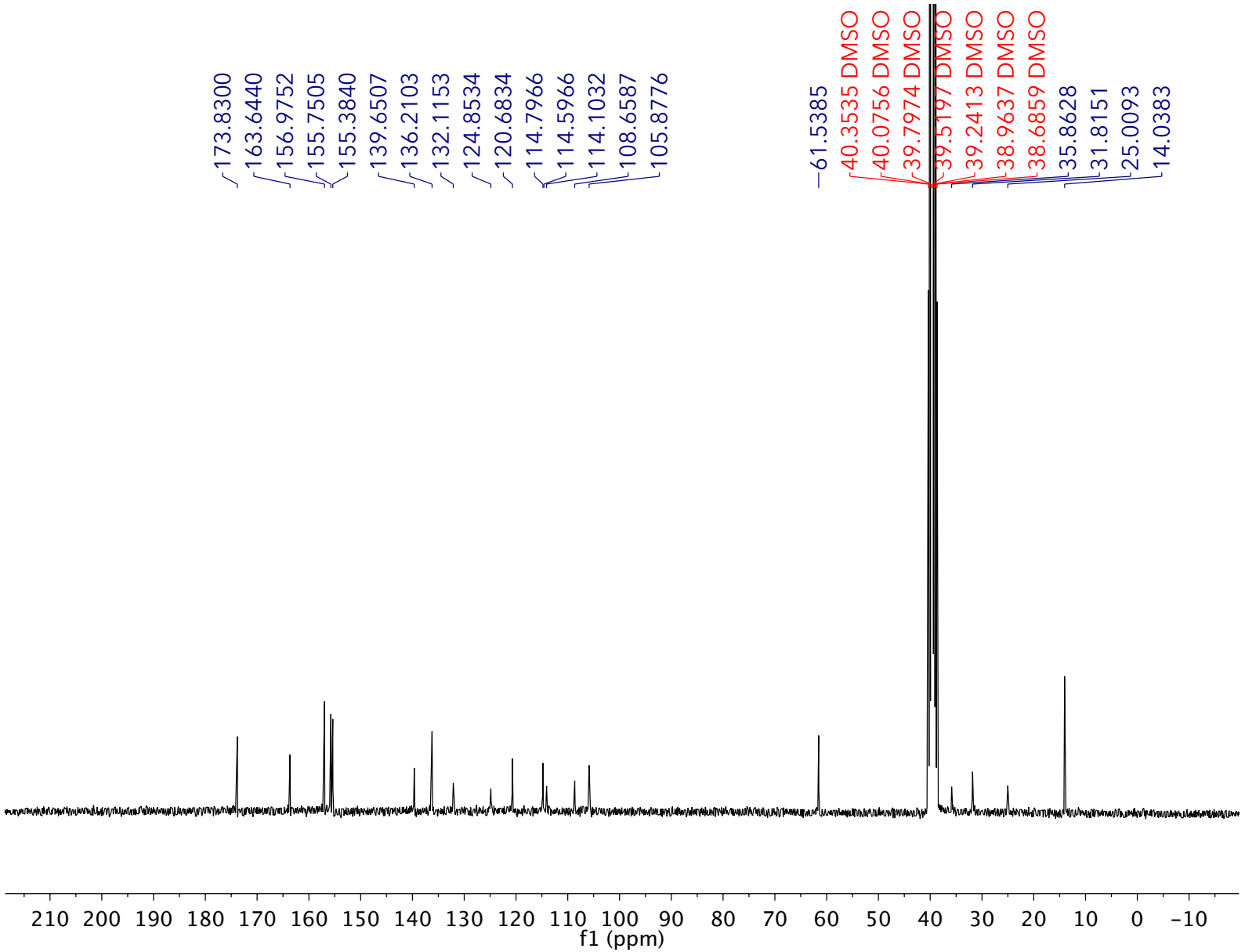

Figure S18: ^{13}C NMR spectrum of tetra-*exo*-ester tetra-acid **f** in DMSO-d_6.

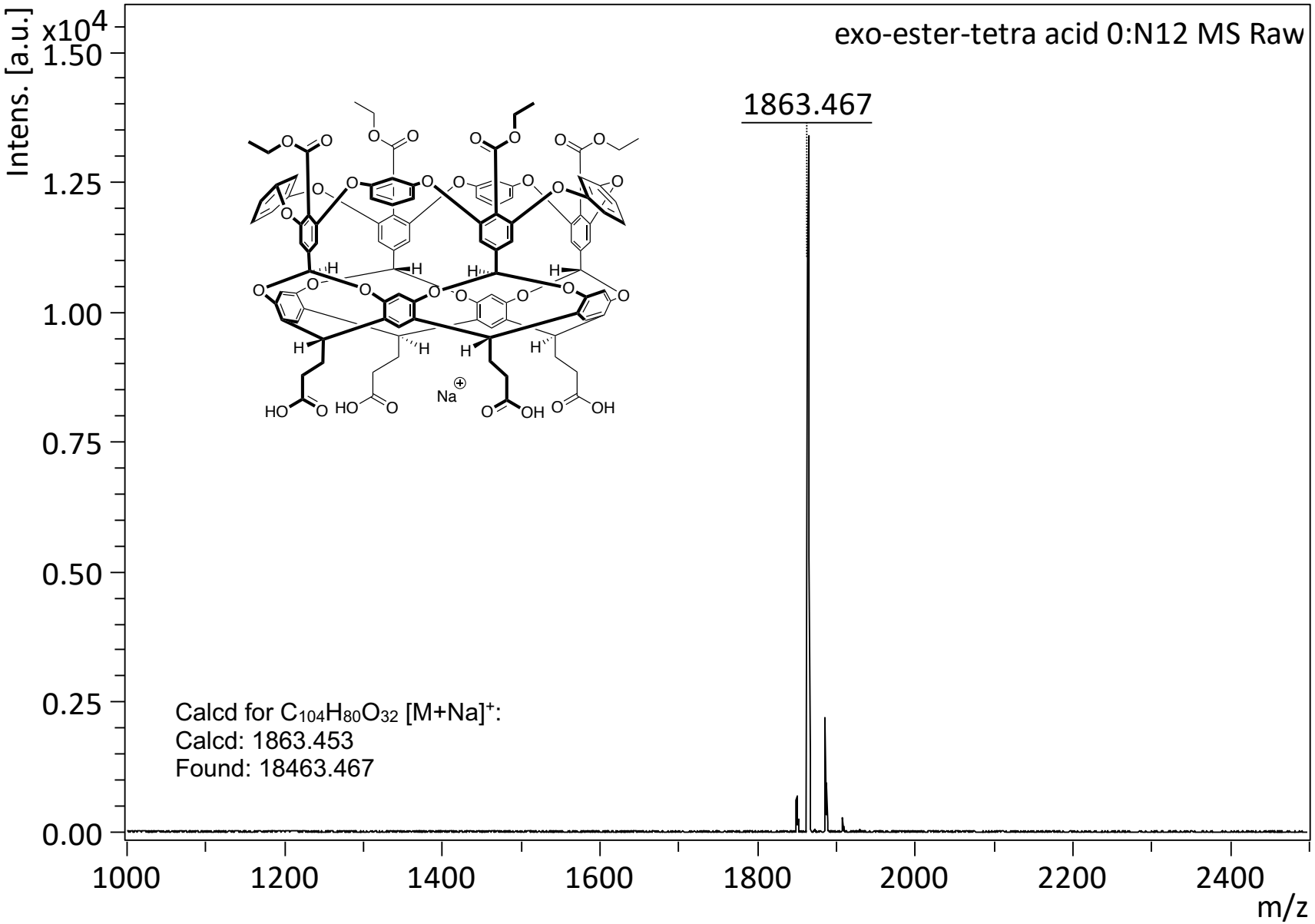

Figure S19: MALDI-TOF MS of tetra-*exo*-ester tetra-acid **f** $[M + Na]^+$ (2:1:1 2 mg ml^{-1} in THF/CHCA/NaTFA).

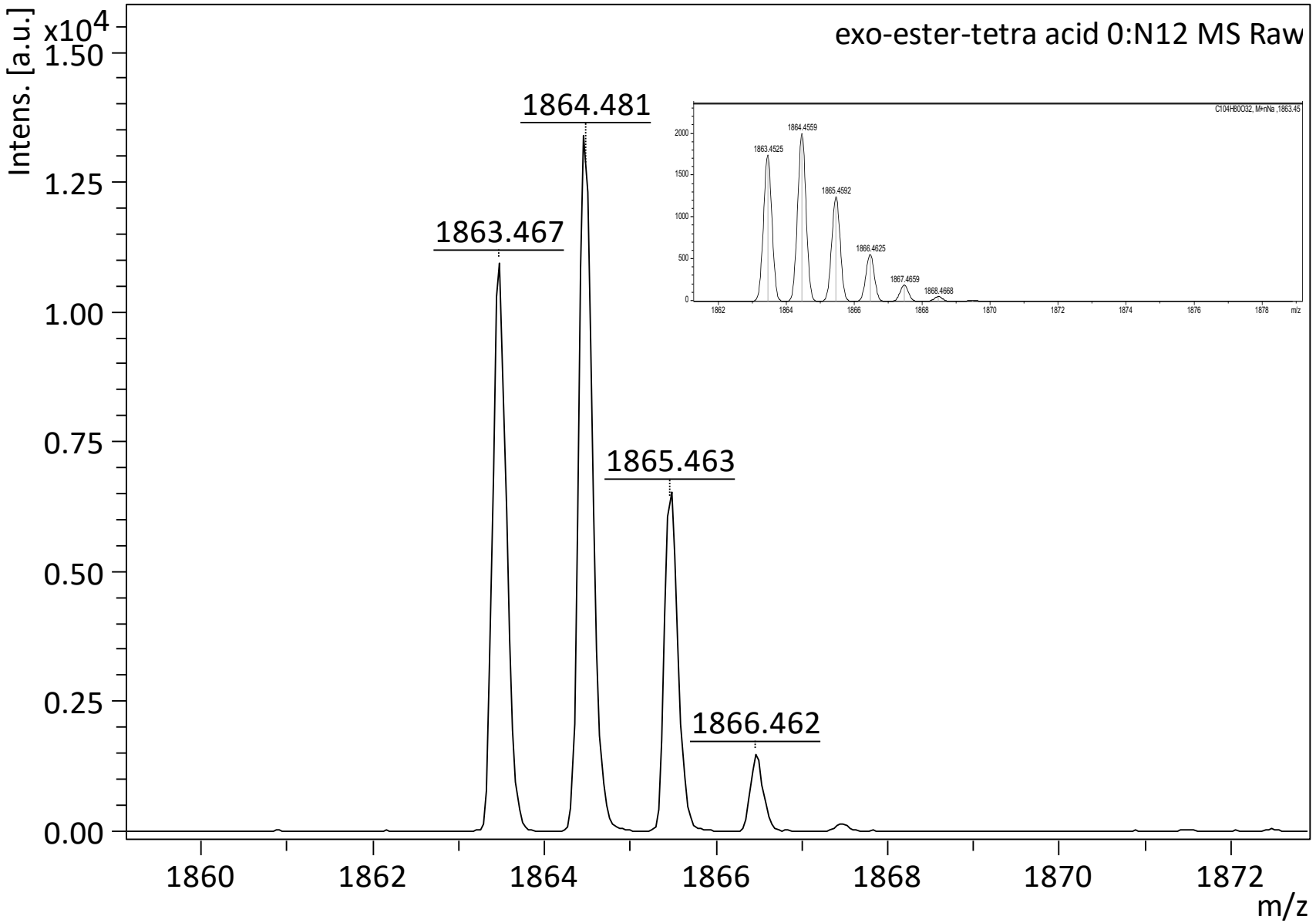

Figure S20: Expanded view of tetra-*exo*-ester tetra-acid **f**, with theoretical calculation insert.

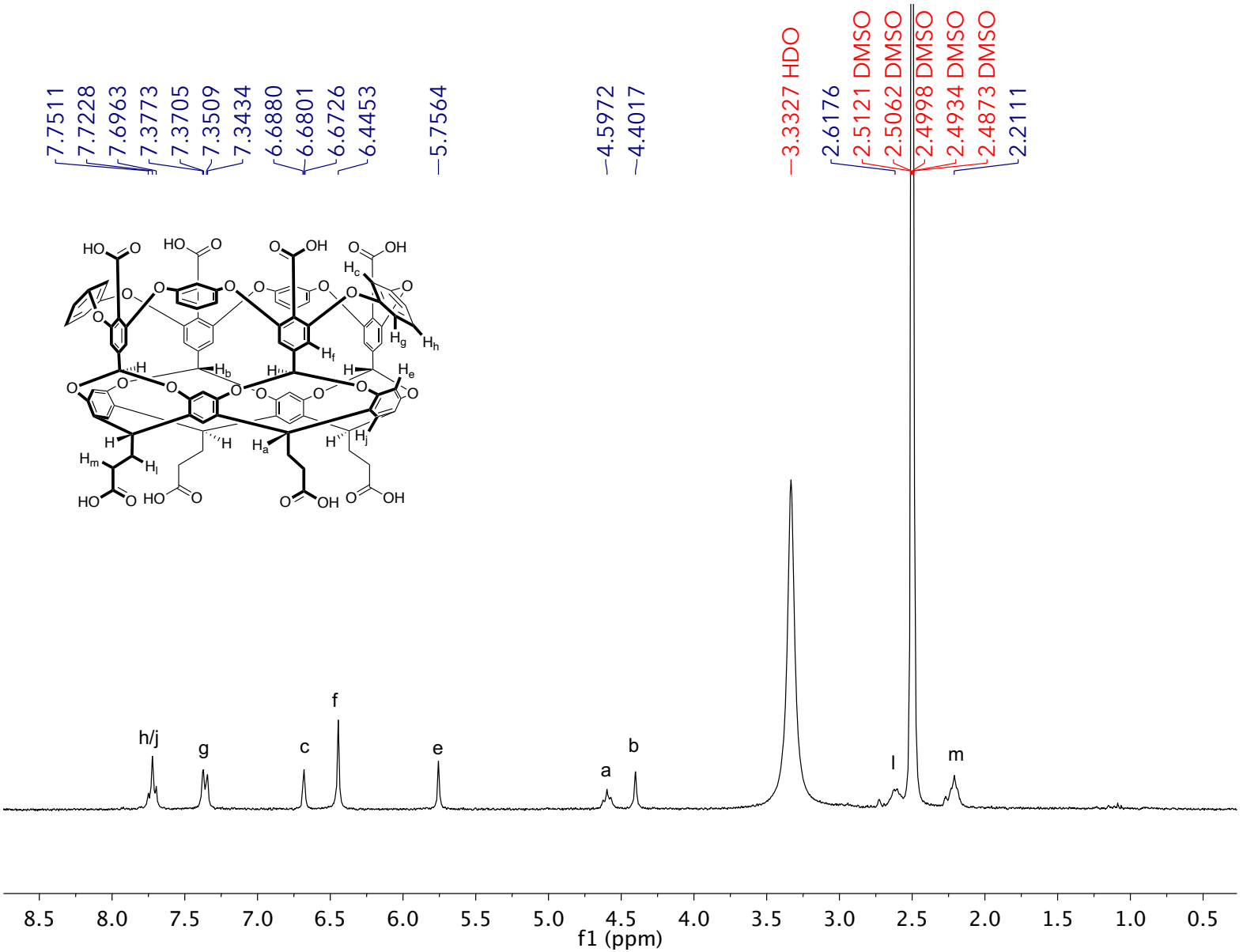

Figure S21: ^{1}H NMR spectrum of *exo*-OA **2** in DMSO-d_6.

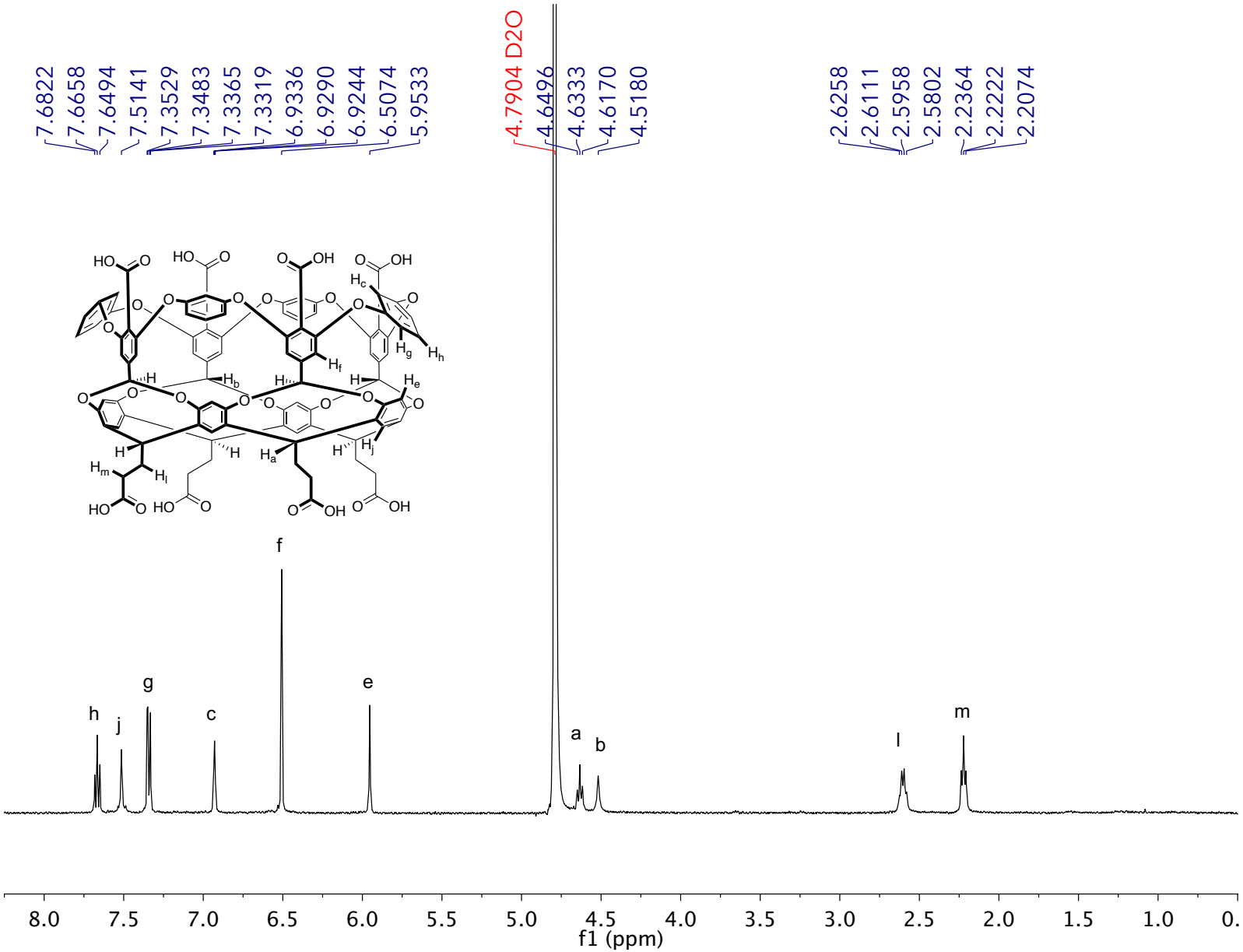

Figure S22: ^{1}H NMR spectrum of 1 mM *exo*-OA **2** in 10 mM pD 11.5 phosphate buffered D_2O.

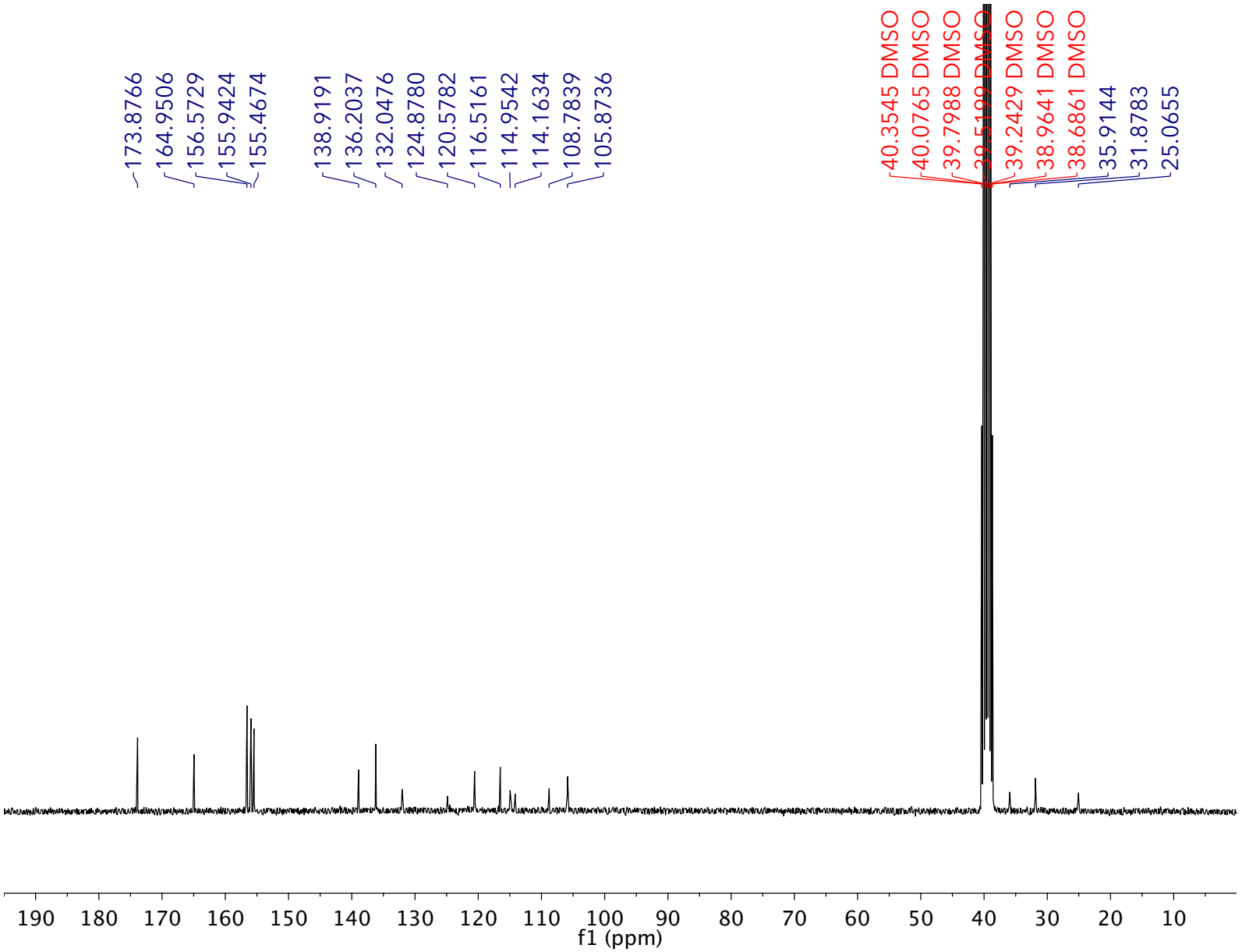

Figure S23: ^{13}C NMR spectrum of *exo*-OA **2** in DMSO-d_6.

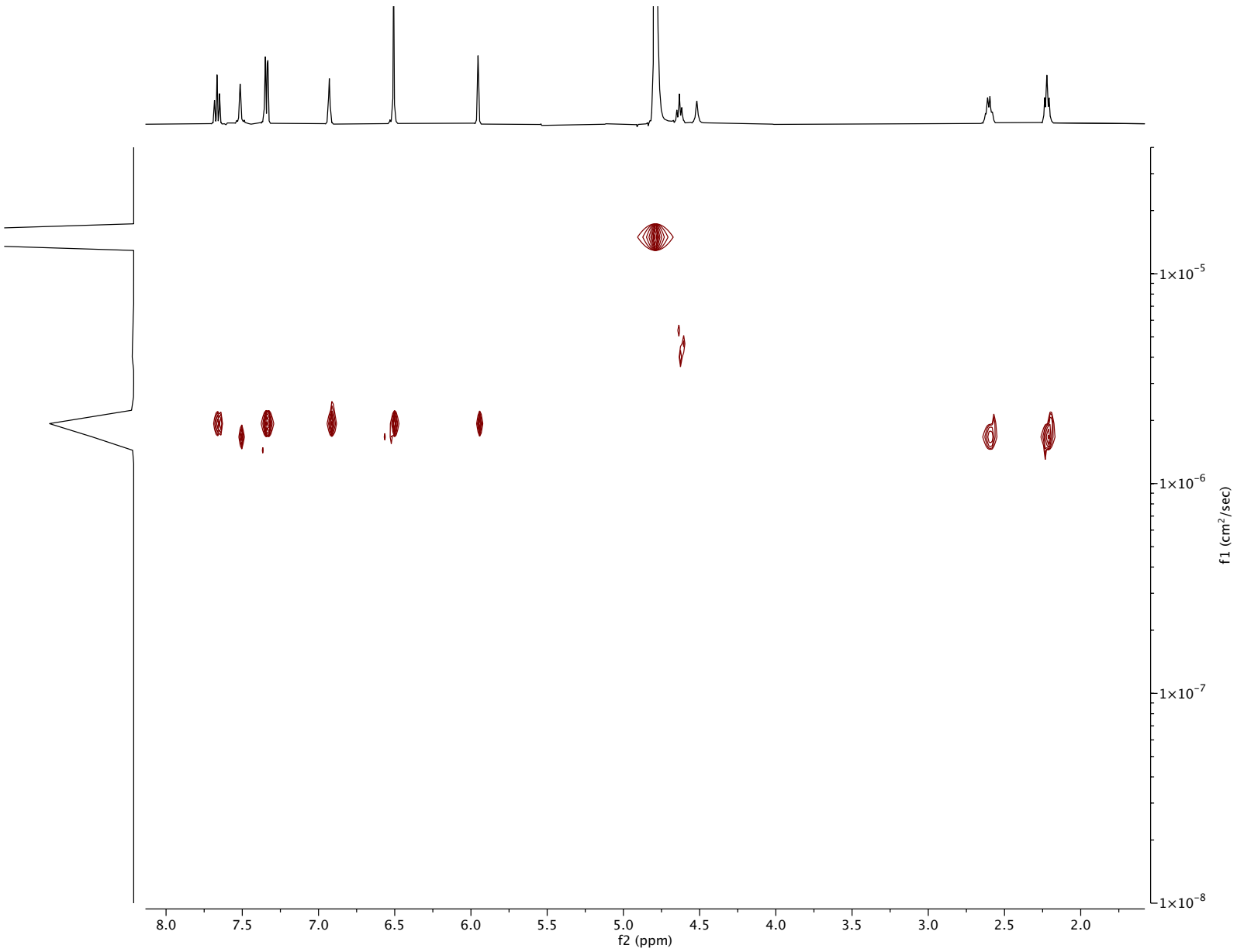

Figure S24: DOSY NMR spectrum of free 1 mM *exo*-OA **2** in 10 mM pD 11.5 phosphate buffered D_2O.

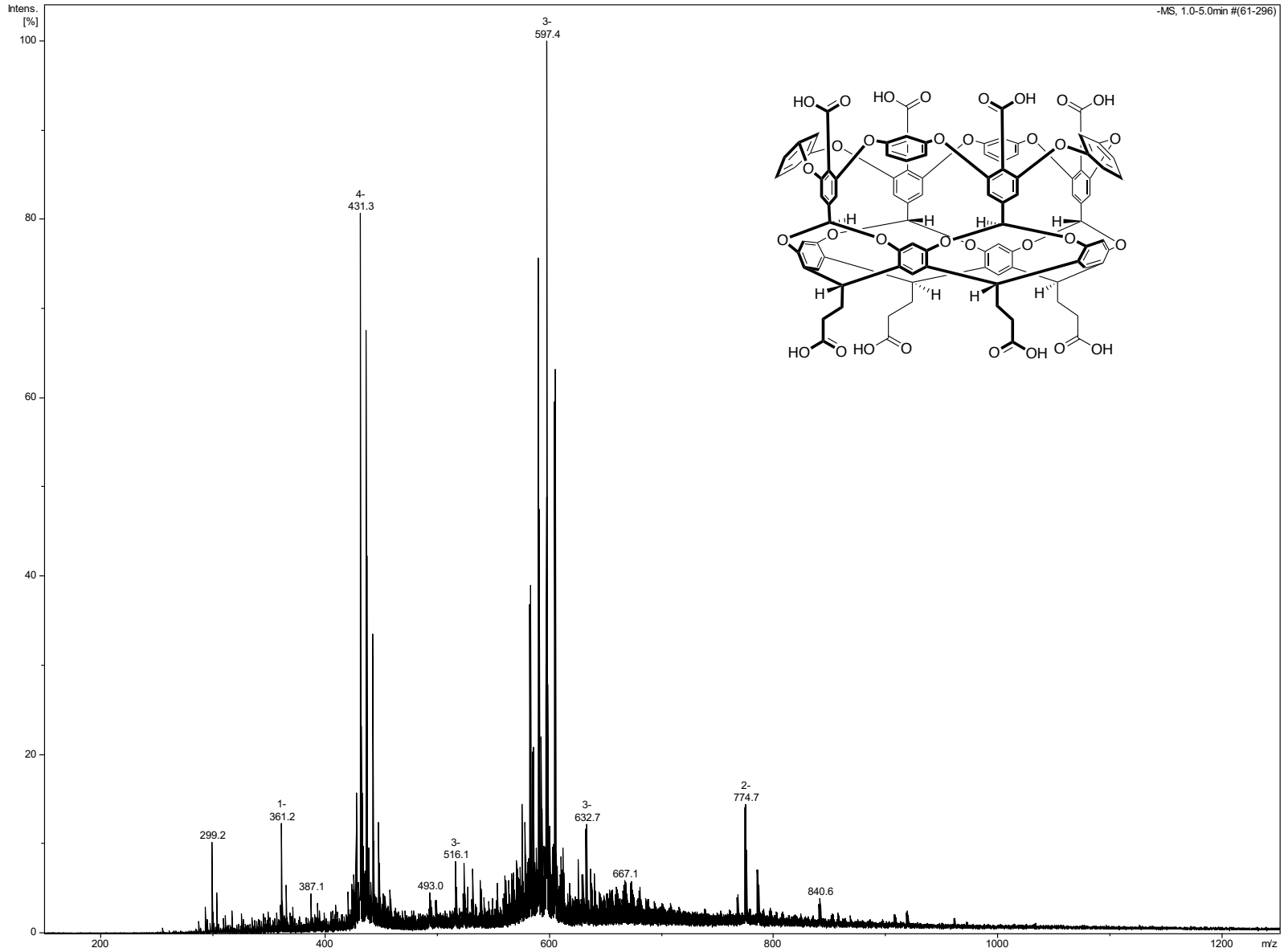

Figure S25: ESI-MS of *exo*-OA 2.

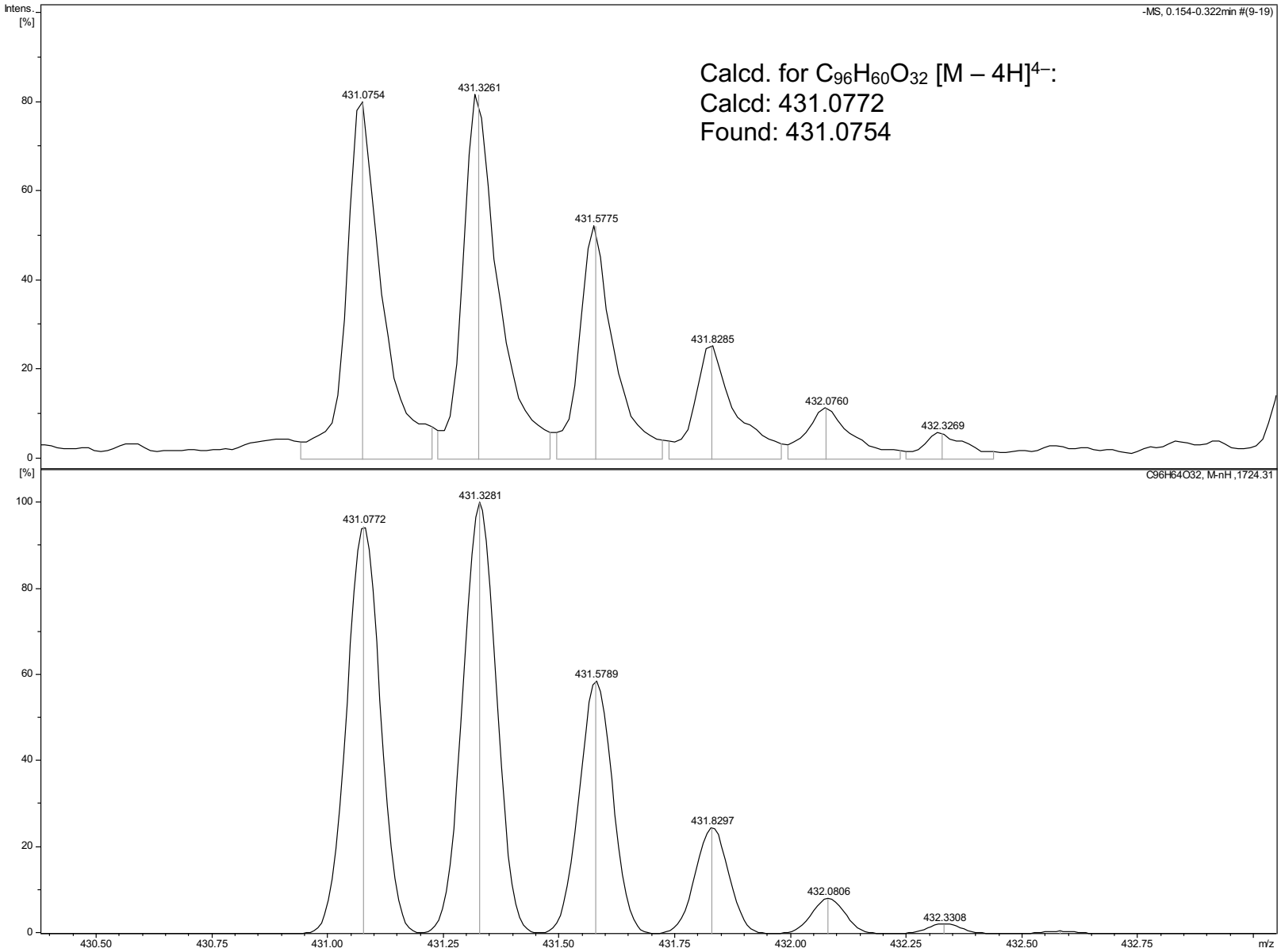

Figure S26: Expanded view of *exo*-OA **2** $[M - 4H]^{4-}$ ($C_{96}H_{60}O_{32}^{4-}$) with theoretical calculation below.

C. Synthesis of G5–G8

Starting from the corresponding primary amines or their hydrochloride salts. the synthesis of the positively charged guest species **G5**-**G8** followed the general procedure as illustrated below,

To a dry flask containing dichloromethane (10 mL) and absolute EtOH (1.1 mL) was added the amine (0.250 g), anhydrous K_2CO_3 (3.3 equiv.), and MeI (3.1 equiv.). The suspension was stirred overnight, after which the solvent was removed under reduced pressure and the residues dried under reduced pressure at rt for 4 h. The resulting residue were then taken up in acetone, sonicated for 5 mins, then filtered. The solvent was removed from the filtrate, the residue dried under reduced pressure at rt for 2 h, then taken up in minimal ultra-pure H_2O. The aqueous solution was passed through a Dowex 1X8 chloride form anion exchange column, and the eluate was lyophilised. The resulting powder was taken up in acetone and filtered. The solvent was removed under reduced pressure and the solids were dried under reduced pressure at rt overnight to yield the trimethylammonium salts as white solids in good (>70%) yields. Spectroscopic data agree with the literature.

β-Phenylethyl(trimethyl)ammonium chloride (G5)[3]
^{1}H NMR (500 MHz, D_2O) δ 3.18 (t, *J* = 8.25 Hz, 2H), 3.20 (s, 9H), 3.59 (tt, *J* = 3.75, 8.5 Hz, 2H), 7.41 (m, 5H).

***n*-Hexyl(trimethyl)ammonium chloride (G6)**[4]
^{1}H NMR (500 MHz, D_2O) δ 0.88 (t, *J* = 7 Hz, 3H), 1.35 (m, 6H), 1.79 (m, 2H), 3.10 (s, 9H), 3.31 (tt, *J* = 3.75, 8.5 Hz, 2H)

***trans*-4-Methylcyclohexyl-1-(trimethyl)ammonium chloride (G7)**[5]
^{1}H NMR (500 MHz, D_2O) δ 0.89 (d, *J* = 6.55 Hz, 3H), 1.06 (dq, *J* = 3.15, 13.1 Hz, 2H), 1.40 (m, 1H), 1.56 (dq, *J* = 3.55, 12.35 Hz, 2H), 1.91 (dt, *J* = 3.15, 13 Hz, 2H), 2.19 (dt, *J* = 3.3, 12.1 Hz, 2H), 3.05 (s, 9H), 3.28 (tt, *J* = 3.45, 12.1 Hz, 1H)

1-Adamantyl(trimethyl)ammonium chloride (G8)[6]
^{1}H NMR (500 MHz, D_2O) δ 1.69 (dd, *J* = 12.8, 24.8 Hz, 6H), 2.07 (s, 6H), 2.31 (s, 3H), 2.99 (s, 9H)

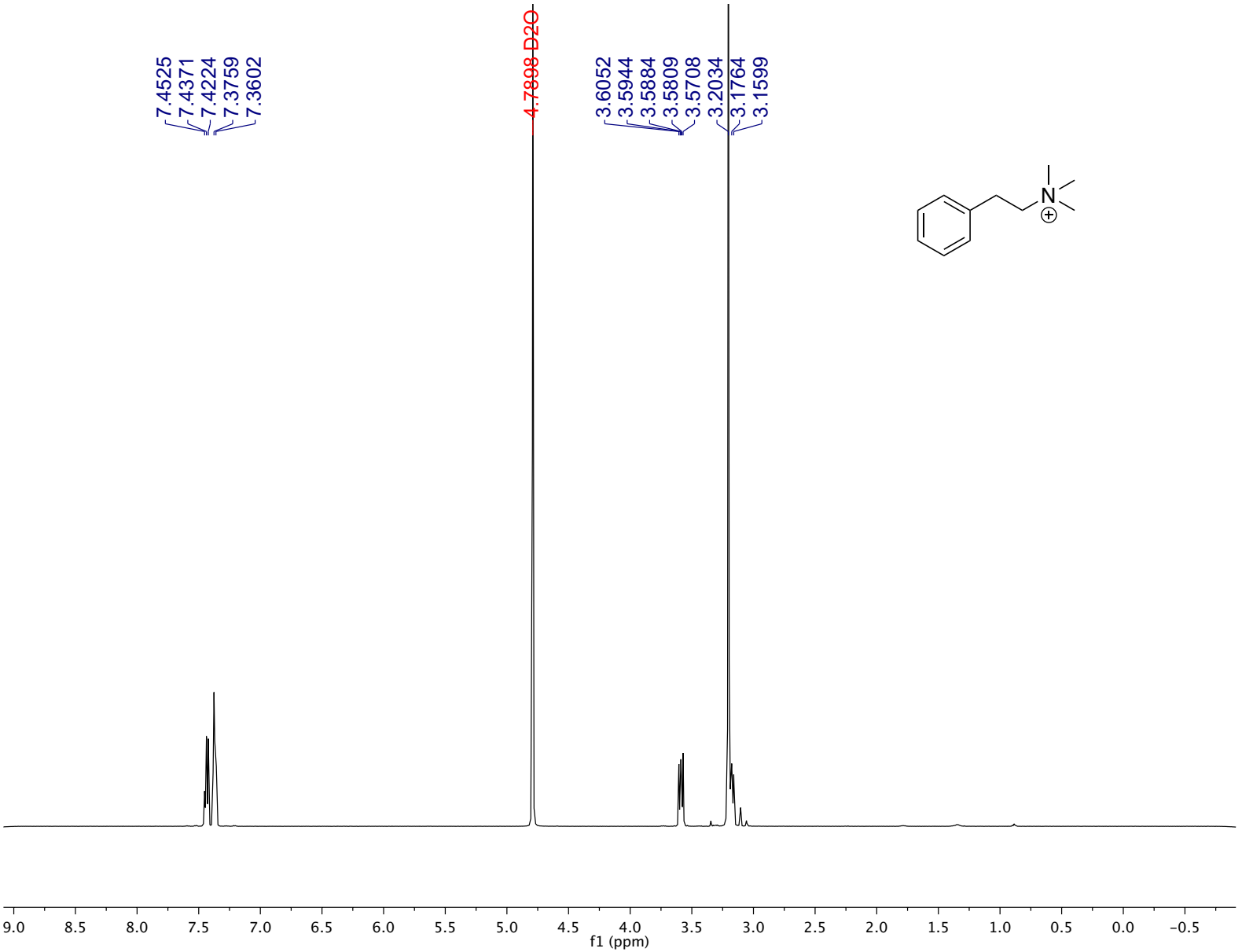

Figure S27: ^{1}H NMR spectrum of G5 in D_2O.

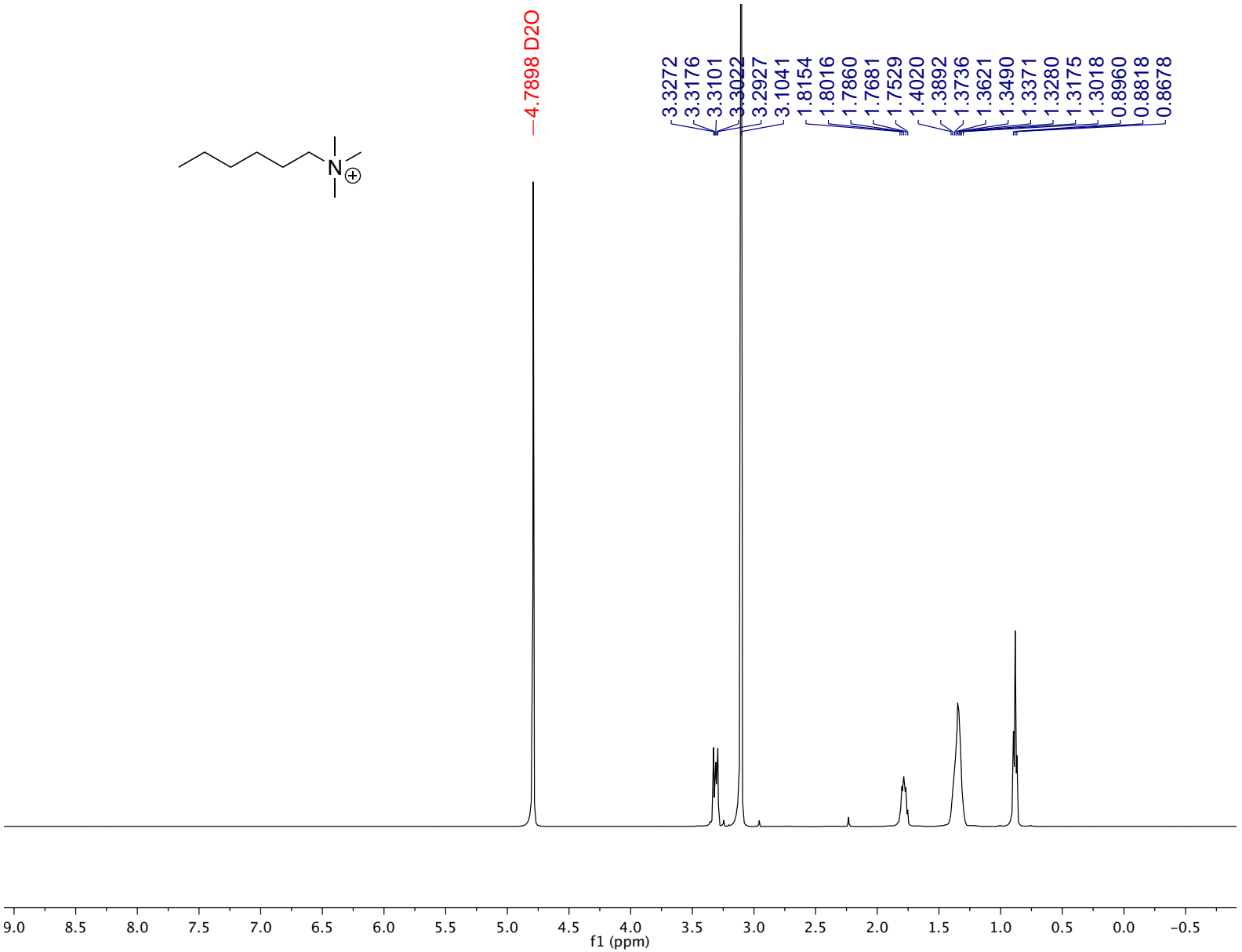

Figure S28: ^{1}H NMR spectrum of G6 in D_2O.

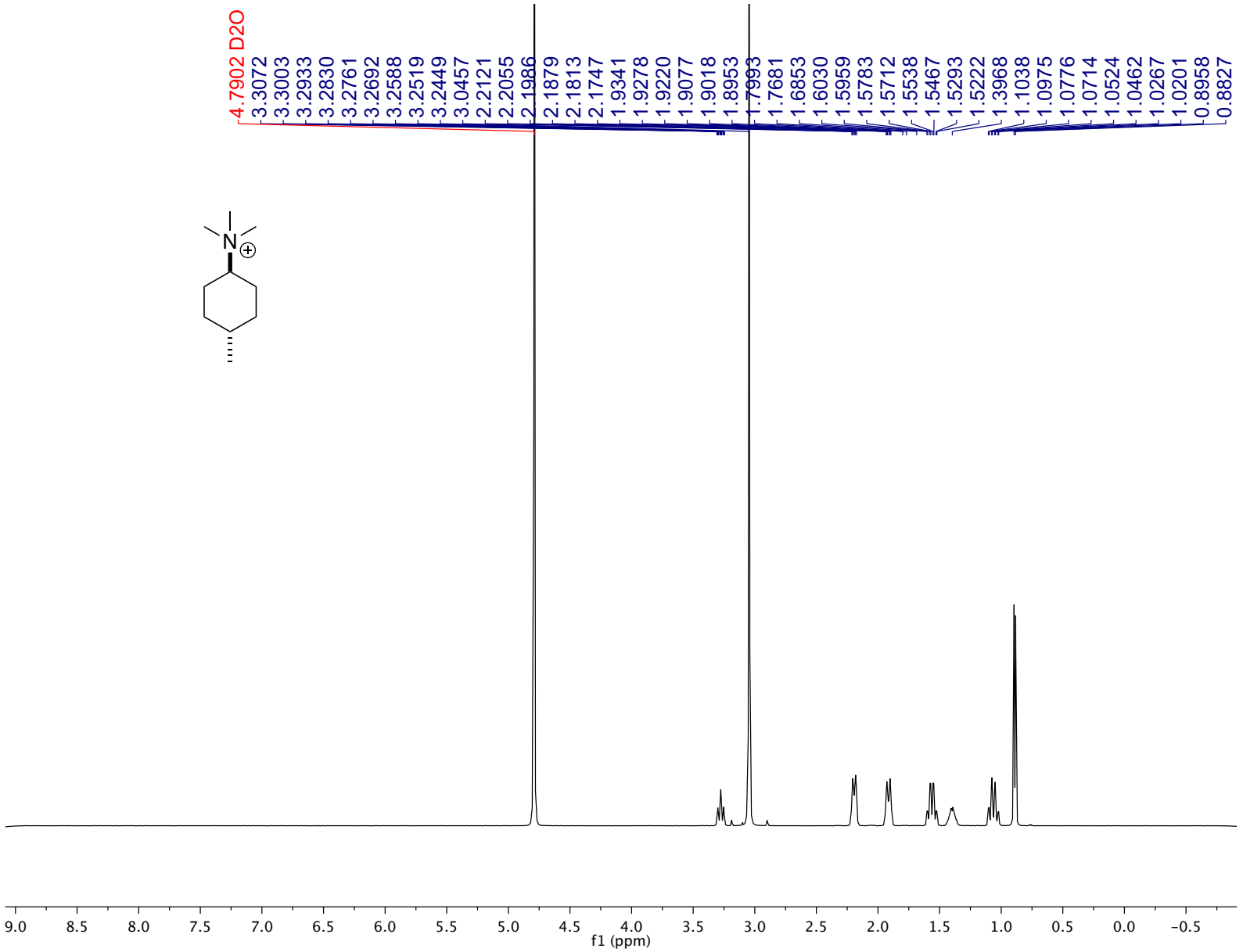

Figure S29: ^{1}H NMR spectrum of G7 in D_2O.

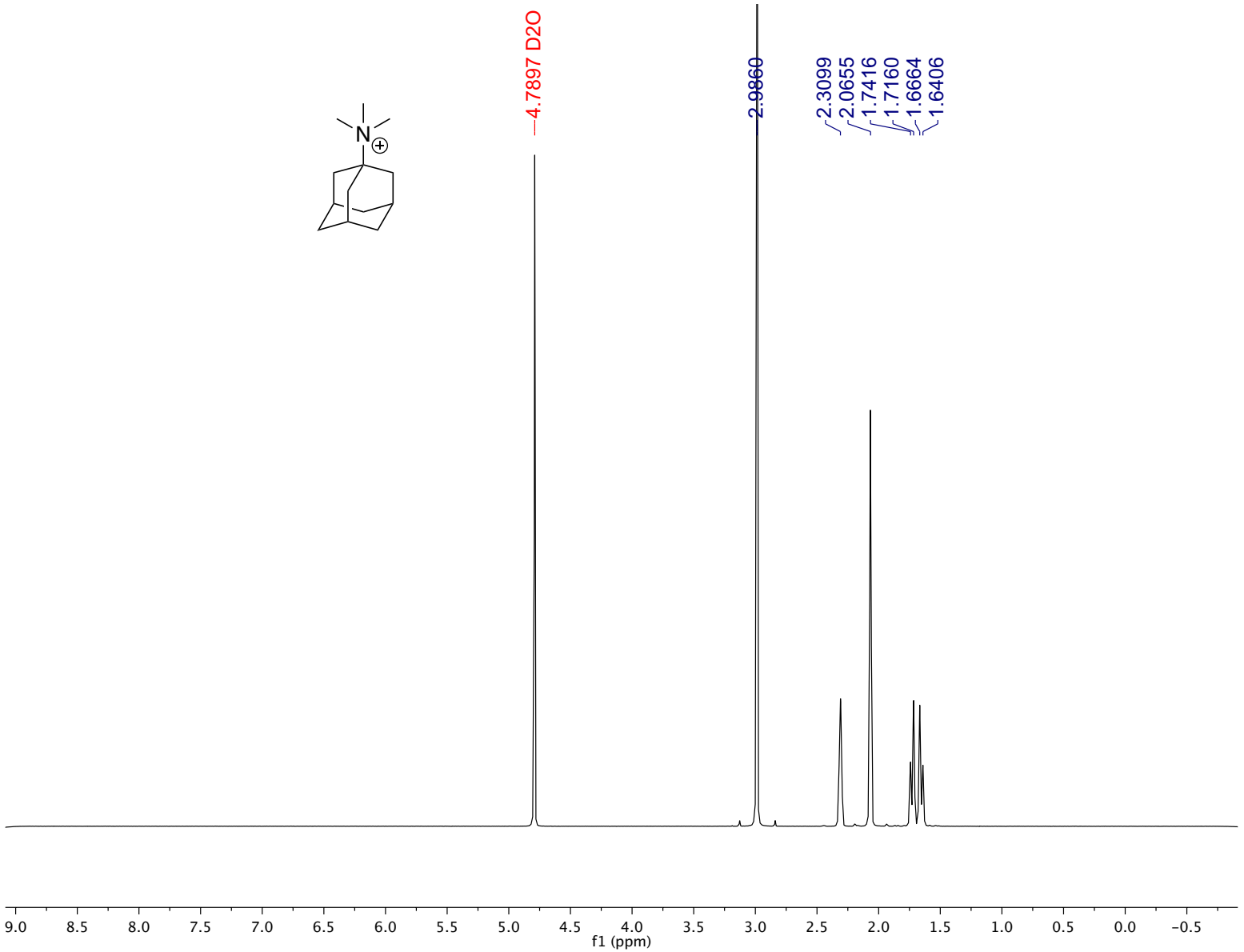

Figure S30: ^{1}H NMR spectrum of G8 in D_2O.

D. Summary of thermodynamic data

Table S1: Thermodynamic data from ITC for the binding of guests **G1**-**G8** with hosts OA **1** and exo-OA **2**. All titrations were performed in 10 mM phosphate buffer at pH 11.5.

Guest	Octa acid 1				Exo-Octa acid 2			
	$\log_{10} K_a$	ΔG (kJ mol^{-1})	ΔH (kJ mol^{-1})	$-T\Delta S$ (kJ mol^{-1})	$\log_{10} K_a$	ΔG (kJ mol^{-1})	ΔH (kJ mol^{-1})	$-T\Delta S$ (kJ mol^{-1})
G1	3.6 ± 1.8	–20.8 ± 0.1[b]	–23.2 ± 0.1[b]	2.4 ± 0.3 [b]	– [c]	– [c]	– [c]	– [c]
G2	5.1 ± 3.0	–28.9 ± 0.1 [b]	–40.2 ± 1.1[b]	11.0 ± 1.0[b]	1.0 ± 0.5	–5.5 ± 1.2	–	–
G3	5.9 ± 4.5	–33.9 ± 0.1	–50.2 ± 0.0	16.3 ± 0.1	2.5 ± 1.6	–14.1 ± 0.3	–25.2 ± 0.6	11.1 ± 0.3
G4	5.0 ± 3.8	–28.3 ± 0.2	–28.0 ± 0.7	–0.3 ± 0.5	2.6 ± 1.3	–15.1 ± 0.1	–30.5 ± 2.9	15.4 ± 2.8
G5	3.5 ± 2.0	–19.8 ± 0.0 [e]	–31.3 ± 0.2 [e]	11.5 ± 0.2[e]	4.1 ± 2.7	–23.3 ± 0.1	–25.8 ± 0.0	2.5 ± 0.1
G6	3.7 ± 2.0	–20.8 ± 0.1[e]	–30.5 ± 1.4[e]	9.6 ± 1.4[e]	4.3 ± 2.5	–24.4 ± 0.0	–13.6 ± 0.1	–10.8 ± 0.1
G7	4.5 ± 3.4	–25.4 ± 0.2	–24.0 ± 0.7	–1.4 ± 0.5	5.1 ± 4.3	–29.2 ± 0.4	–20.8 ± 0.3	–8.4 ± 0.2
G8	6.0 ± 4.8	–34.5 ± 0.1	–32.7 ± 0.8	–1.7 ± 0.6	5.6 ± 3.9	–32.1 ± 0.0	–21.1 ± 0.2	–11.0 ± 0.1

[a] Data and errors in this table were determined as follows. The ΔH and ΔG values were obtained by carrying out at least three separate experiments, averaging each set of data, and calculating the respective standard deviation. These average ΔH and ΔG values were then used to calculate an average $-T\Delta S$, and the corresponding standard deviation calculated using the standard equation for the propagation of uncertainties for subtraction.
[b] Data for this host-guest combination was determined as part of SAMPL4 in 50 mM borate. [7]
[c] No binding observed.
[d] Determined by ^{1}H NMR spectroscopy.
[e] Data for this host-guest combination was determined as part of SAMPL5 in 50 mM phosphate.[8]

E. Isothermal titration calorimetry (ITC): instrumentation

Isothermal Titration Calorimetric (ITC) experiments within this study were performed at 298 K using a VP-ITC MicroCalorimeter from Microcal, USA. Integrated heat data obtained for the titrations were fitted using the MicroCal-Origin 7.0 software package. All titrations were carried out in 10 mM sodium phosphate buffer of pH ~ 11.5 at 25 °C. Before each experiment, both host and guest solutions were degassed for 2–5 min to eliminate air bubbles. The injection volumes for all titrations used the computer-controlled injection procedure of guest solution into host solution. The injection volumes used for each titration are detailed in the next section.

The binding for most host-guest pairs gave adequate heats of injection such that general ITC titration procedures could be followed. However, in the case of **2**–**G3** and **2**–**G4**, the Wiseman "*c*" values (c = [host] × K_a) were less than ideal (i.e., < 5),[9] and modification procedures defined by Turnbull[10] and Tellinghuisen[11] were followed. Thus, variable titrant volumes were used to deliver a large excess of guest with the stoichiometry parameter N fixed to 1. We have used the same modification procedures previously.[8, 12] Moreover, because the heats of complexation were relatively low, higher concentrations of the guest titrant were required which necessitated guest dilution reference titrations (guest injected into buffer solution without host) to be carried out and subtracted from the host-guest titration.

All the ITC titrations exhibited clear thermal responses and gave an excellent fit for a 1:1 complex model. All titrations were run in triplicate, and good reproducibility of K_a and ΔH values with the experimental error between runs less than 5%, and $-T\Delta S$ values less than 15% (Table S1).

F. ITC Experimental parameters

Each host-guest system required specific conditions to fit within the instrumental limitations inherent of ITC. Specifically, the concentrations for host and guest, injection procedure, and DP (Differential Power) value used for each host-guest pair is listed below.

Hexanoic acid (G1):

OA **1**: DP = 25 μcal s^{-1}. The ITC titration experiment utilized a 30-injection procedure of 15 mM guest solution titrated into 1 mM host solution. V_1 = 2.0 μL; $V_2 – V_{30}$ = 9.0 μL

ExoOA: ITC could not be used for this host-guest combination because of insufficient heat of complexation. As an alternate, an NMR titration experiment was carried out on 0.50 mM host solution in 10 mM pD 11.5 phosphate-buffered D_2O. A 200 mM guest solution in the same buffer solution was titrated into the host solution. $V_1 – V_3$ = 2 μL; V_4 = 4 μL; $V_5 – V_8$ = 5 μL; V_9 = 20 μL; V_{10} = 10 μL; V_{11} = 50 μL.

4-Chlorobenzoic acid (G2):

OA **1**: DP = 25 μcal s^{-1}. The ITC titration experiment utilized a 29-injection procedure of a 1.5 mM guest solution titrated into a 0.15 mM host solution. V_1 = 2.0 μL; $V_2 – V_{29}$ = 9.0 μL.

ExoOA: ITC could not be used for this host-guest combination because of insufficient heat of complexation. As an alternate, an NMR titration experiment was carried out on 0.50 mM host solution in 10 mM pD 11.5 phosphate-buffered D_2O. A 250 mM guest solution in the same buffer solution was titrated into the host solution, and the host signals were recorded and globally fitted using a 1:1 NMR model[13] on Bindfit.[14] $V_1 – V_3$ = 2 μL; V_4 = 4 μL; $V_5 – V_8$ = 5 μL; V_9 = 20 μL; V_{10} = 10 μL.

(*S*)-(–)-Perillic Acid (G3):
OA **1**: DP = 25 µcal s^{-1}. The ITC titration experiment utilized a 33-injection procedure of a 5 mM guest solution titrated into a 0.5 mM host solution. V_1 = 2.0 µL; $V_2 – V_7$ = 5.0 µL; $V_8 – V_{12}$ = 7.0 µL; $V_{13} – V_{33}$ = 9.0 µL.

exo-OA **2**: DP = 30 µcal s^{-1}. The ITC titration experiment utilized a 33-injection procedure of a 80 mM guest solution titrated into a 1.0 mM host solution: V_1 = 2.0 µL; $V_2 – V_5$ = 5.0 µL; $V_6 – V_9$ = 7.0 µL; V10 – V33 = 9.0 µL.

(*S*)-(–)-Citronellic acid (G4):
OA **1**: DP = 25 µL s^{-1}. The ITC titration experiment utilized a 33-injection procedure of a 5.0 mM guest solution titrated into a 0.50 mM host solution. V_1 = 2.0 µL; $V_2 – V_7$ = 5.0 µL; $V_8 – V_{12}$ = 7.0 µL; $V_{13} – V_{33}$ = 9.0 µL.

exo-OA **2**: DP = 35 µcal s^{-1}. The ITC titration experiment utilized a 33-injection procedure of a 100 mM guest solution titrated into a 1 mM host solution. V_1 = 2.0 µL; $V_2 – V_7$ = 5.0 µL; $V_8 – V_{12}$ = 7.0 µL; $V_{13} – V_{33}$ = 9.0 µL.

β-Phenylethyl(trimethyl)ammonium chloride (G5):
OA **1**: DP = 15 µcal s^{-1}. The ITC titration experiment utilized a 28-injection procedure of a 7.5 mM guest solution titrated into a 0.15 mM host solution: V_1 = 1.0 µL; V_2 = 2.0 µL; V_3 = 2.5 µL; V_4 = 3.0 µL; V_5 = 3.5 µL; V_6 = 4.0 µL; V_7 = 4.5 µL; V_8 = 5.0 µL; V_9 = 5.5 µL; V_{10} = 6.0 µL; V_{11} = 6.5 µL; V_{12} = 7.0 µL; V_{13} = 7.5 µL; V_{14} = 8.0 µL; V_{15} = 8.5 µL; V_{16} = 9.0 µL; V_{17} = 9.5 µL; V_{18} = 10.0 µL; V_{19} = 10.5 µL; V_{20} = 11.0 µL; V_{21} = 11.5 µL; V_{22} = 12.0 µL; V_{23} = 12.5 µL; V_{24} = 13.0 µL; V_{25} = 13.5 µL; V_{26} = 14.0 µL; V_{27} = 14.5 µL; V_{28} = 15.0 µL.

exo-OA **2**: DP = 20. The ITC titration experiment utilized a 28-injection procedure of a 10 mM guest solution titrated into a 1 mM host solution: V_1 = 3.0 µL; $V_2 – V_4$ = 6.0 µL; $V_5 – V_{28}$ = 9.0 µL.

***n*-Hexyl(trimethyl)ammonium chloride (G6):**
OA **1**: DP = 15 µcal s^{-1}. The ITC titration experiment utilized a 28-injection procedure of a 7.5 mM guest solution titrated into a 0.15 mM host solution: V_1 = 1.0 µL; V_2 = 2.0 µL; V_3 = 2.5 µL; V_4 = 3.0 µL; V_5 = 3.5 µL; V_6 = 4.0 µL; V_7 = 4.5 µL; V_8 = 5.0 µL; V_9 = 5.5 µL; V_{10} = 6.0 µL; V_{11} = 6.5 µL; V_{12} = 7.0 µL; V_{13} = 7.5 µL; V_{14} = 8.0 µL; V_{15} = 8.5 µL; V_{16} = 9.0 µL; V_{17} = 9.5 µL; V_{18} = 10.0 µL; V_{19} = 10.5 µL; V_{20} = 11.0 µL; V_{21} = 11.5 µL; V_{22} = 12.0 µL; V_{23} = 12.5 µL; V_{24} = 13.0 µL; V_{25} = 13.5 µL; V_{26} = 14.0 µL; V_{27} = 14.5 µL; V_{28} = 15.0.

exo-OA **2**: DP = 15 µcal s^{-1}. The ITC titration experiment utilized a 28-injection procedure of a 7.5 mM guest solution titrated into a 0.15 mM host solution: V_1 = 1.0 µL; V_2 = 2.0 µL; V_3 = 2.5 µL; V_4 = 3.0 µL; V_5 = 3.5 µL; V_6 = 4.0 µL; V_7 = 4.5 µL; V_8 = 5.0 µL; V_9 = 5.5 µL; V_{10} = 6.0 µL; V_{11} = 6.5 µL; V_{12} = 7.0 µL; V_{13} = 7.5 µL; V_{14} = 8.0 µL; V_{15} = 8.5 µL; V_{16} = 9.0 µL; V_{17} = 9.5 µL; V_{18} = 10.0 µL; V_{19} = 10.5 µL; V_{20} = 11.0 µL; V_{21} = 11.5 µL; V_{22} = 12.0 µL; V_{23} = 12.5 µL; V_{24} = 13.0 µL; V_{25} = 13.5 µL; V_{26} = 14.0 µL; V_{27} = 14.5 µL; V_{28} = 15.0.

***trans*-4-Methylcyclohexyl(trimethyl)ammonium chloride (G7):**
OA **1**: DP = 10 µcal s^{-1}. The ITC titration experiment used a 28-injection procedure of 1.5 mM guest solution into 0.15 mM host solution. The following variable injection volumes were used: V_1 = 3.0; $V_2 – V_{28}$ = 9.0 µL.

exo-OA **2**: DP = 10 µcal s^{-1}. The ITC titration experiment used a 28-injection procedure of 1.5 mM guest solution into 0.15 mM host solution. The following variable injection volumes were used: V_1 = 3.0 µL; $V_2 – V_{28}$ = 9.0 µL.

1-Adamantyl(trimethyl)ammonium chloride (G8):
OA **1**: DP = 10 µcal s^{-1}. The ITC titration experiment used a 28-injection procedure of 1.5 mM guest solution into 0.15 mM host solution. The following variable injection volumes were used: V_1 = 3.0 µL; $V_2 – V_{28}$ = 9.0 µL.

exo-OA **2**: DP = 10 µcal s^{-1}. The ITC titration experiment used a 28-injection procedure of 1.5 mM guest solution into 0.15 mM host solution. The following variable injection volumes were used: V_1 = 3.0 µL; $V_2 – V_{28}$ = 9.0 µL.

G. ITC results

The figures below show an example thermogram and binding curve of one titration experiment for each host–guest pair.

Hexanoic acid (G1)

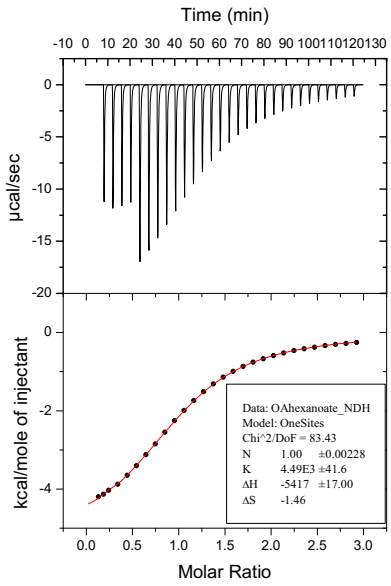

Figure S31: ITC thermogram and 1:1 binding fit for **OA**–**G1** complexation. A 15 mM solution of **G1** was titrated into a 1.0 mM solution of **OA** equilibrated at 25 °C. Both host and guest were in 10 mM phosphate buffer, pH 11.5.

4-Chlorobenzoic acid (G2)

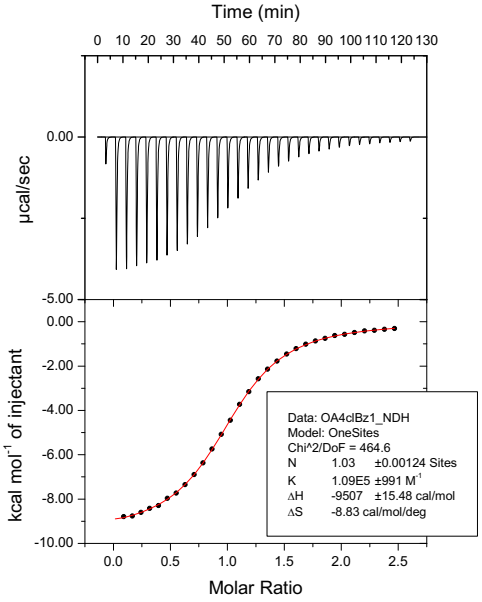

Figure S32: ITC thermogram and 1:1 binding fit for **OA–G2** complexation. A 1.5 mM solution of **G2** was titrated into a 0.15 mM solution of **OA** equilibrated at 25 °C. Both host and guest were in 10 mM phosphate buffer, pH 11.5.

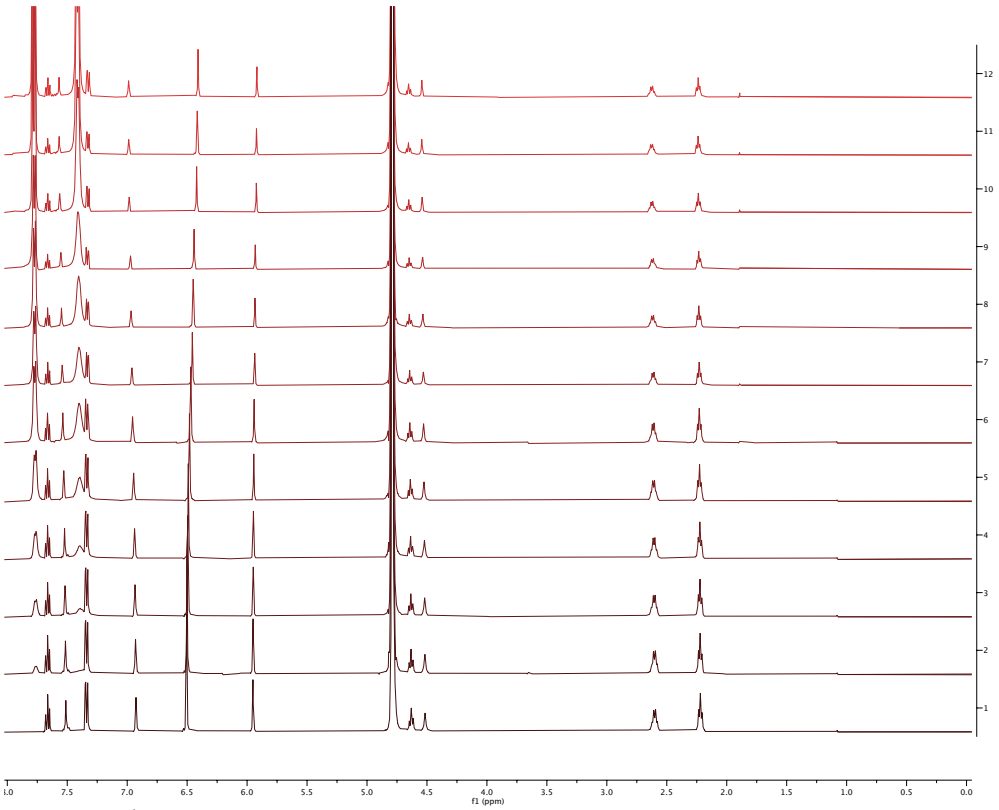

Figure S33: (*left*) ^{1}H NMR titration stack showing the addition of 250 mM **G2** into a 0.5 mM solution of ***exo*-OA**. Spectrum 1 is of the free host, while spectrum 12 is at the end of the titration at 60 equiv. **G2**.

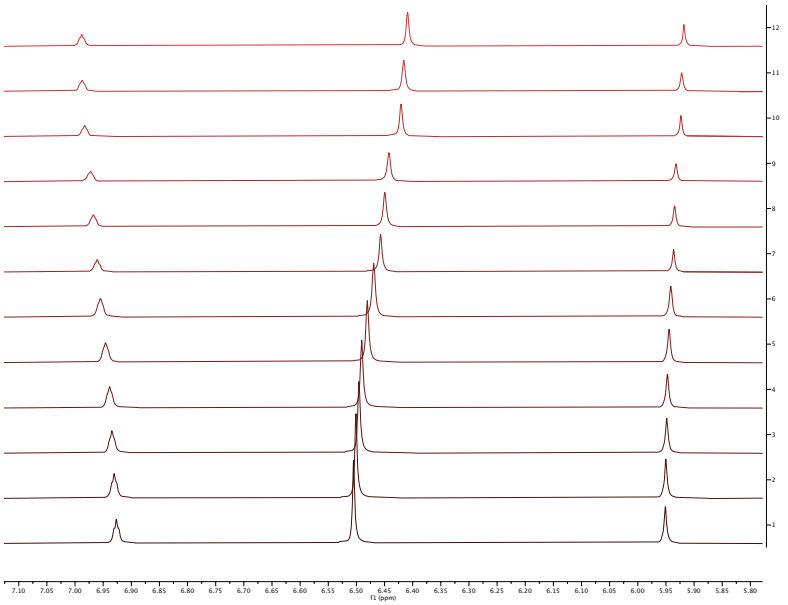

Figure S34: Host region between 5.80 – 7.10 ppm showing the shifting of ***exo*-OA** host peaks (H_c, H_f and H_e, see Figure S1) as a function of **G2**. Spectrum 1 is of free ***exo*-OA**, and spectrum 12 is at the end of the titration at 60 equiv. **G2.**

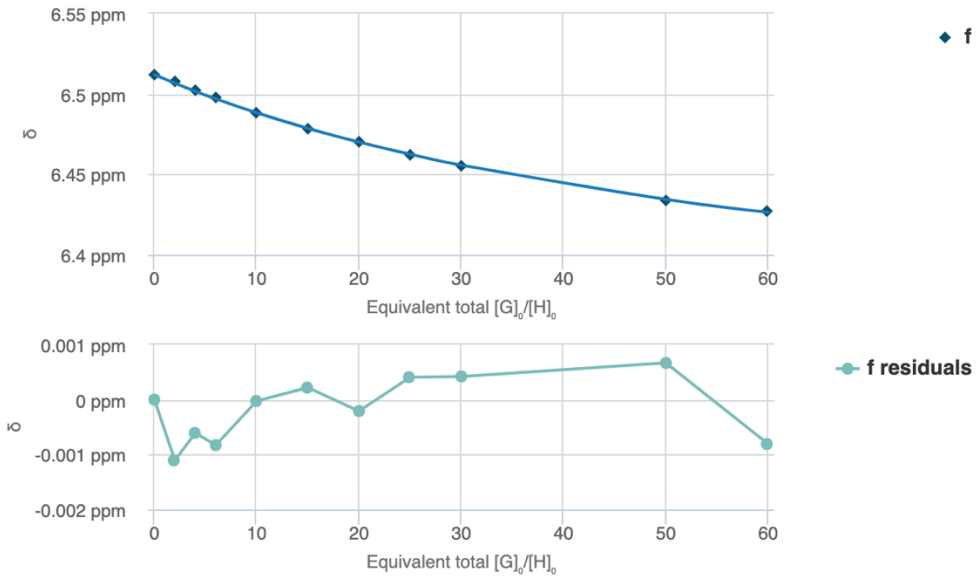

Figure S35: Representative fitting curve (*top*) of the titration of 250 mM **G2** to 0.5 mM ***exo*-OA** and the corresponding residuals (*bottom*). Curve and residuals were calculated using the online BindFit software.[13, 14]

Perillic acid (G3)

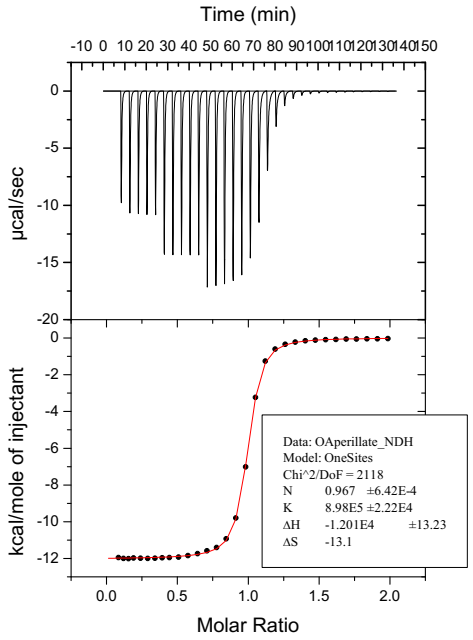

Figure S36: ITC thermogram and 1:1 binding fit for **OA**–**G3** complexation. A 5.0 mM solution of **G3** was titrated into a 0.5 mM solution of **OA** equilibrated at 25 °C. Both host and guest were in 10 mM phosphate buffer, pH 11.5.

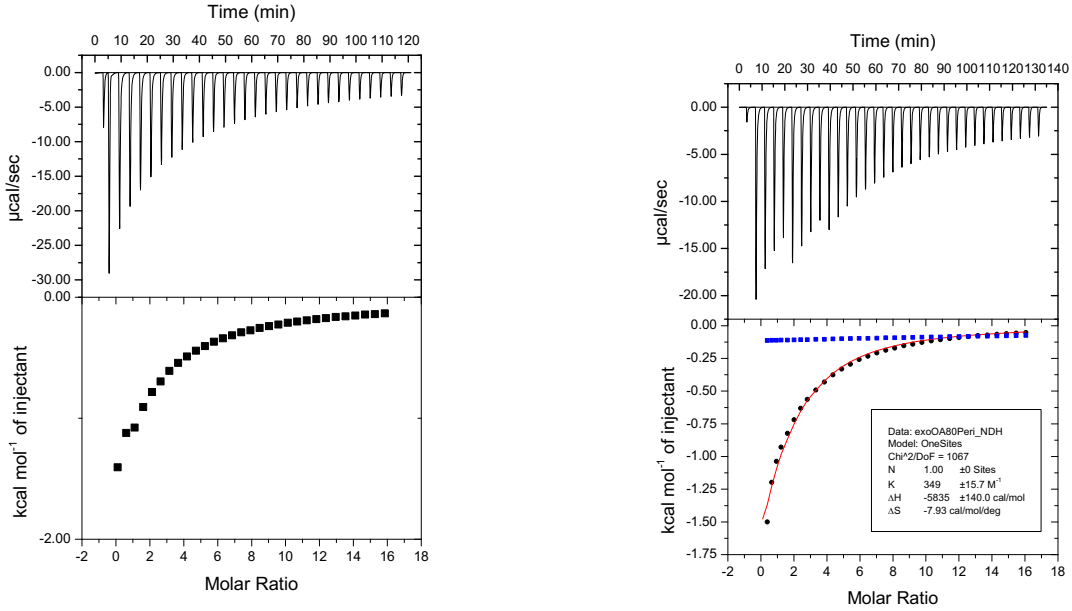

Figure S37: ITC thermogram and 1:1 binding fit for **exo-OA**–**G3** complexation. An 80 mM solution of **G3** was titrated into a 1.0 mM solution of **exo-OA** equilibrated at 25 °C. Both host and guest were in 10 mM phosphate buffer, pH 11.5. (left) Raw thermogram; (right) thermogram after subtraction of guest injections into buffer solution.

Citronellic acid (G4)

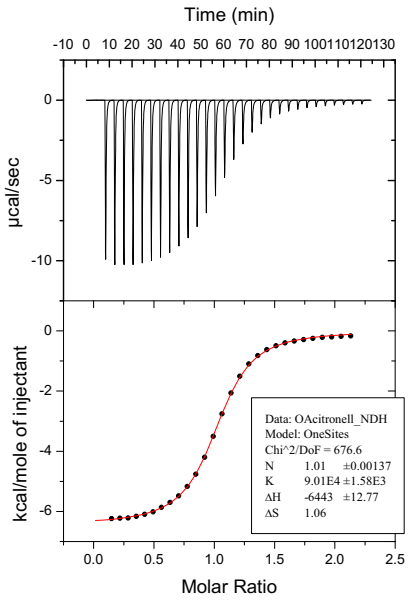

Figure S38: ITC thermogram and 1:1 binding fit for **OA**–**G4** complexation. A 5 mM solution of **G4** was titrated into a 0.5 mM solution of **OA** equilibrated at 25 °C. Both host and guest were in 10 mM phosphate buffer, pH 11.5.

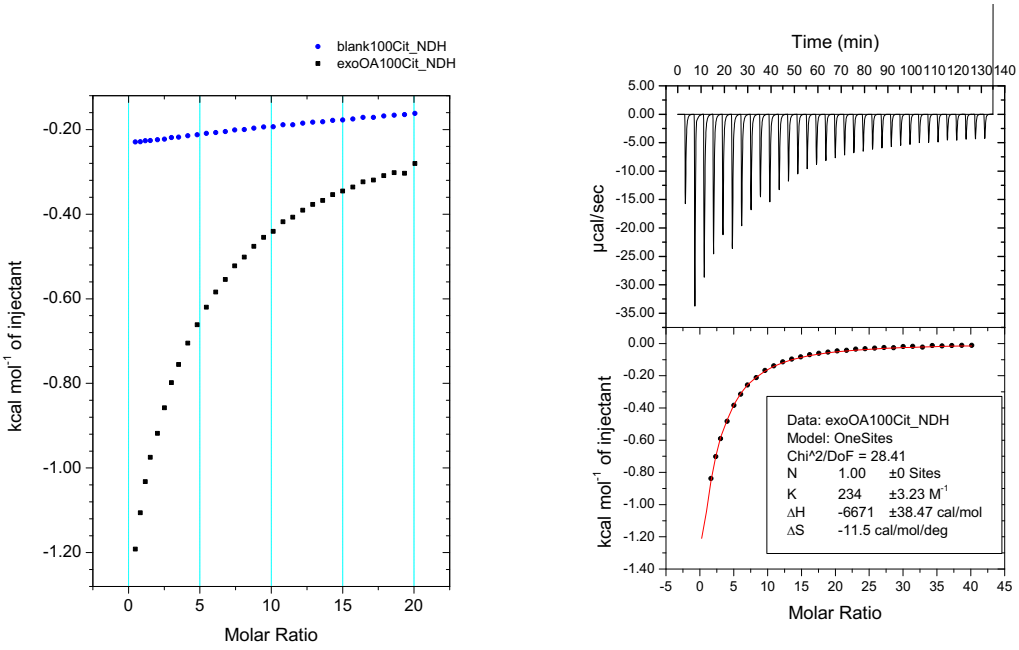

Figure S39: ITC thermogram and 1:1 binding fit for **exo-OA**–**G4**complexation. A 100 mM solution of **G4** was titrated into a 1.0 mM solution of **exo-OA** equilibrated at 25 °C. Both host and guest were in 10 mM phosphate buffer, pH 11.5. (left) Raw thermogram; (right) thermogram after subtraction of guest injections into buffer.

β-Phenylethyl(trimethylammonium) chloride (G5)

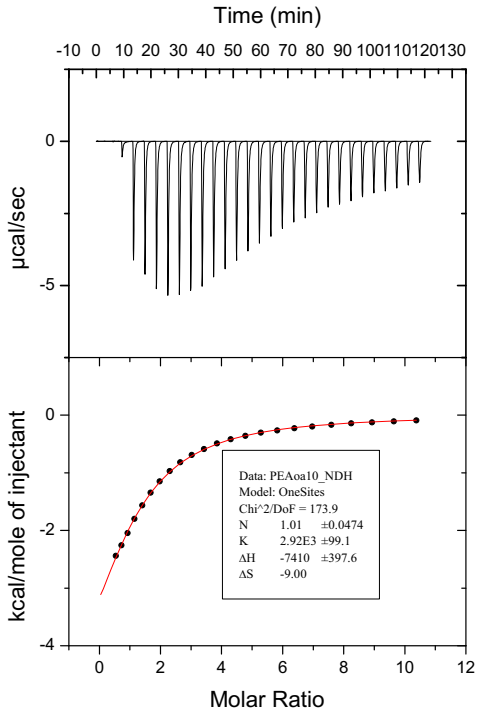

Figure S40: ITC thermogram and 1:1 binding fit for **OA**–**G5** complexation. A 7.5 mM solution of **G5** was titrated into a 0.5 mM solution of **OA** equilibrated at 25 °C. Both host and guest were in 10 mM phosphate buffer, pH 11.5.

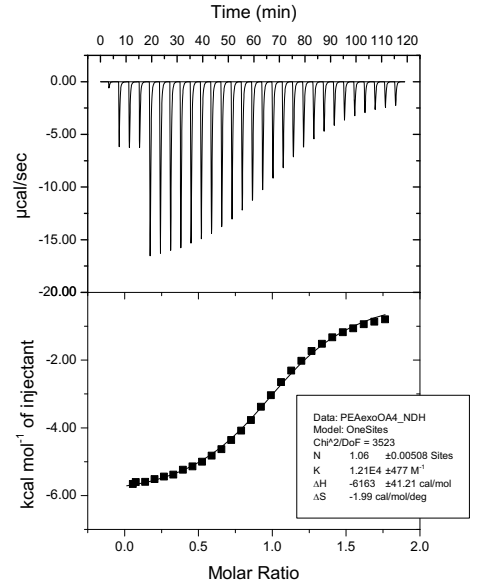

Figure S41: ITC thermogram and 1:1 binding fit for **exo-OA**–**G5** complexation. A 10 mM solution of **G5** was titrated into a 1.0 mM solution of **exo-OA** equilibrated at 25 °C. Both host and guest were in 10 mM phosphate buffer, pH 11.5.

n-Hexyl(trimethyl)ammonium chloride (G6)

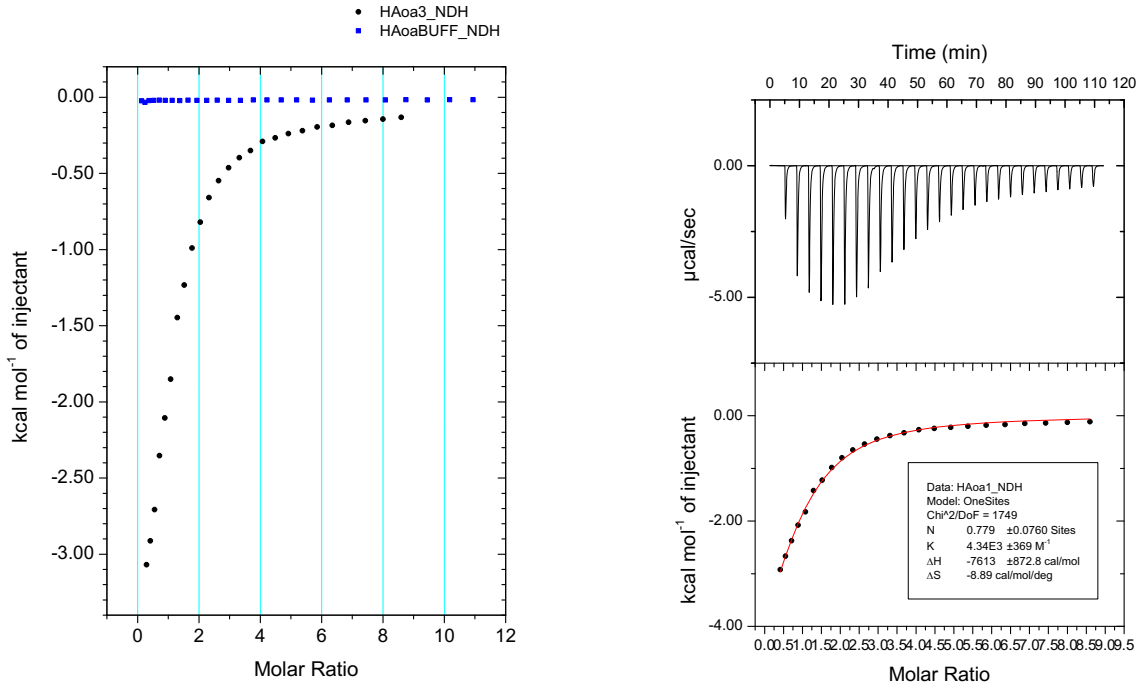

Figure S42: ITC thermogram and 1:1 binding fit for **OA**–**G6** complexation. A 7.5 mM solution of **G6** was titrated into a 0.15 mM solution of **OA** equilibrated at 25 °C. Both host and guest were in 10 mM phosphate buffer, pH 11.5. (left) Raw thermogram; (right) thermogram after subtraction of guest injections into buffer.

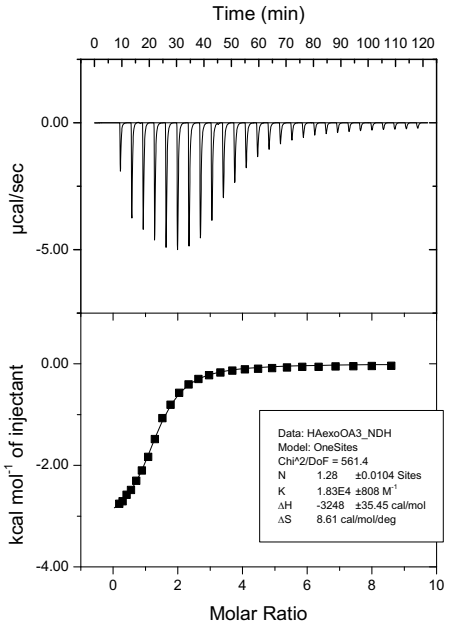

Figure S43: ITC thermogram and 1:1 binding fit for **exo-OA**–**G6** complexation. A 7.5 mM solution of **G6** was titrated into a 0.15 mM solution of **exo-OA** equilibrated at 25 °C. Both host and guest were in 10 mM phosphate buffer, pH 11.5.

trans-4-Methylcyclohexyl(trimethyl)ammonium chloride (G7)

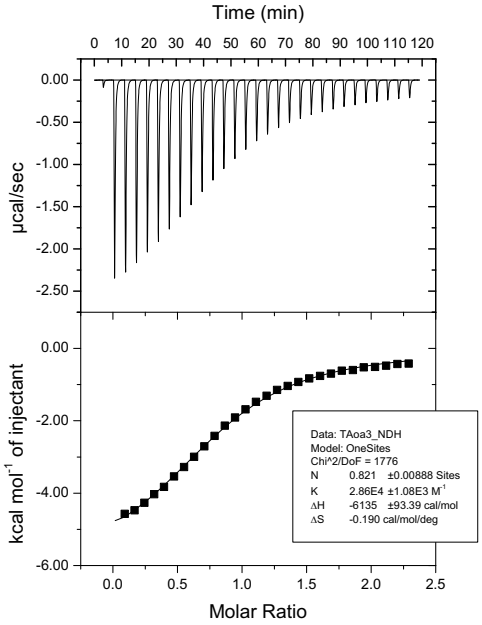

Figure S44: ITC thermogram and 1:1 binding fit for **OA**–**G7** complexation. A 1.5 mM solution of **G7** was titrated into a 0.5 mM solution of **OA** equilibrated at 25 °C. Both host and guest were in 10 mM phosphate buffer, pH 11.5.

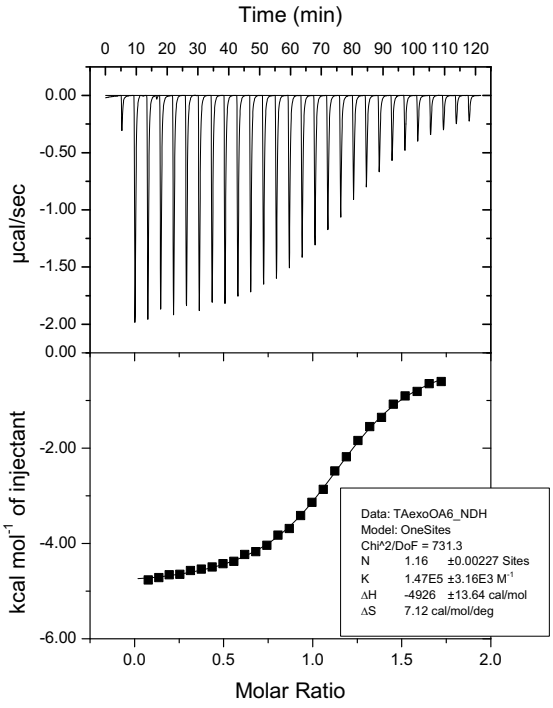

Figure S45: ITC thermogram and 1:1 binding fit for **exo-OA**–**G7** complexation. A 0.15 mM solution of **G7** was titrated into a 0.15 mM solution of **exo-OA** equilibrated at 25 °C. Both host and guest were in 10 mM phosphate buffer, pH 11.5.

1-Adamantyl(trimethylammonium) chloride (G8)

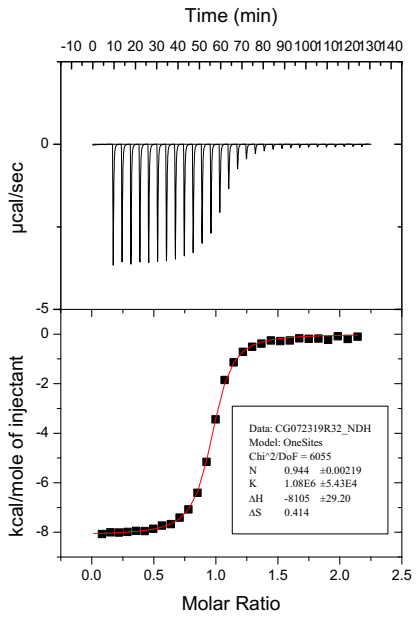

Figure S46: ITC thermogram and 1:1 binding fit for **OA–G8** complexation. A 1.5 mM solution of **G8** was titrated into a 0.15 mM solution of **OA** equilibrated at 25 °C. Both host and guest were in 10 mM phosphate buffer, pH 11.5.

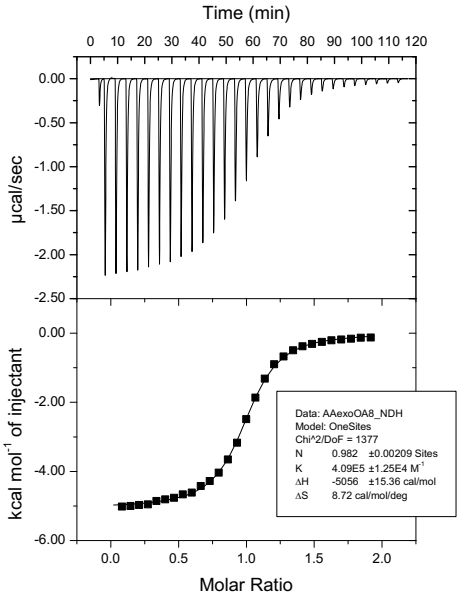

Figure S47: ITC thermogram and 1:1 binding fit for **exo-OA**–**G8** complexation. A 1.5 mM solution of **G8** was titrated into a 0.15 mM solution of **exo-OA** equilibrated at 25 °C. Both host and guest were in 10 mM phosphate buffer, pH 11.5.

H. One-to-one binding of guests to *exo*-OA via NMR

Evidence for binding of **G5–G7** could not be obtained by NMR as the exchange rate between the free and bound states are on the timescale of the NMR experiment. Even for the strongest binding guest to ***exo*-OA** (**G8**) the binding is slightly faster than the NMR experiment timescale. Upon addition of one equivalent of **G8** to ***exo*-OA**, the signals that correspond to H_b of the host and $-NMe_3$ of the guest integrate to a 4:9 ratio, indicating the formation of a 1:1 host–guest complex (**Figure S50**).

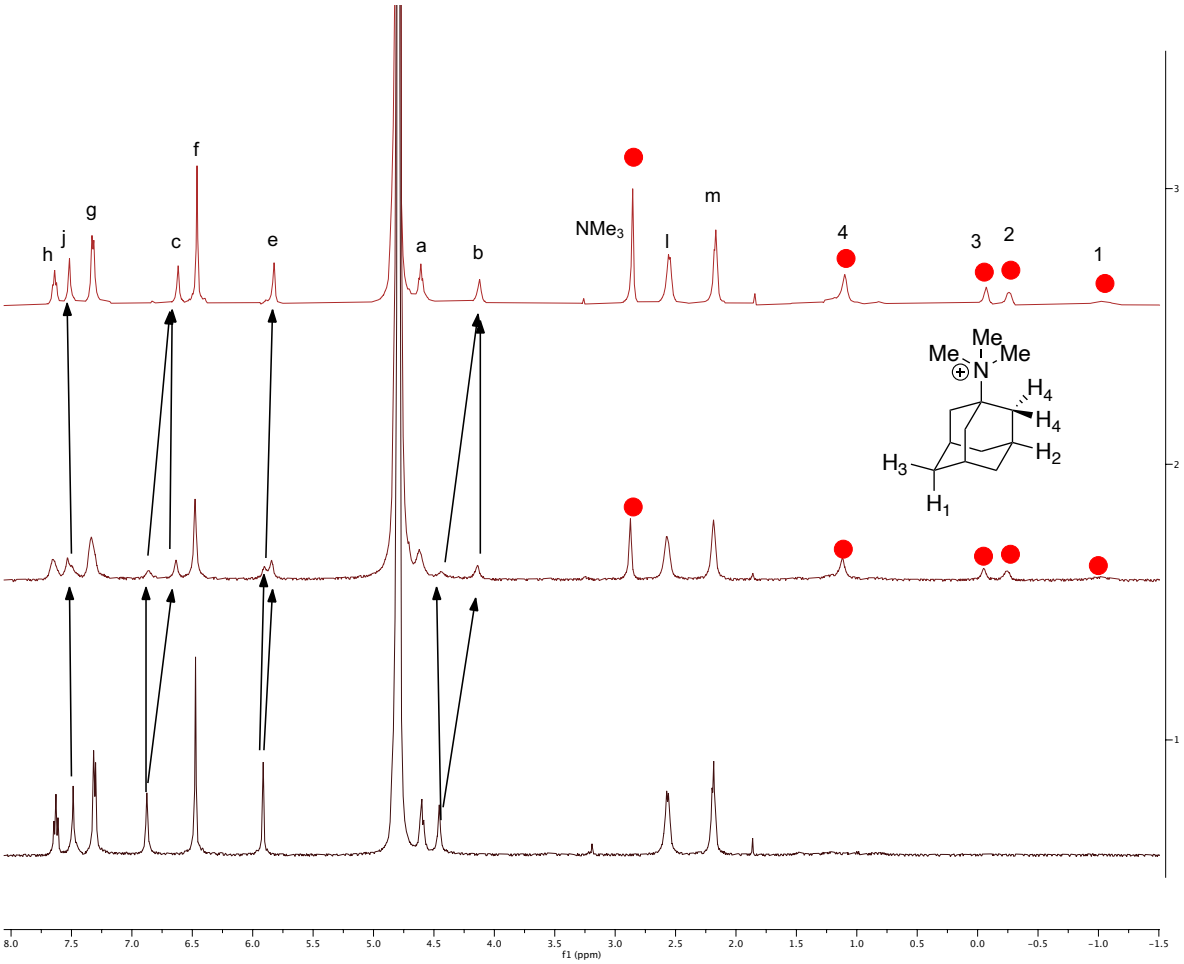

Figure S48: ^{1}H NMR stack of the addition of **G8** to ***exo*-OA**. Spectrum 1 is of free ***exo*-OA**; 2 is of 0.5 equiv. **G8** into ***exo*-OA**; 3 is of 1 equiv. **G8** into ***exo*-OA**. Arrows indicate shifts in host peaks, red circles indicate bound guest peaks.

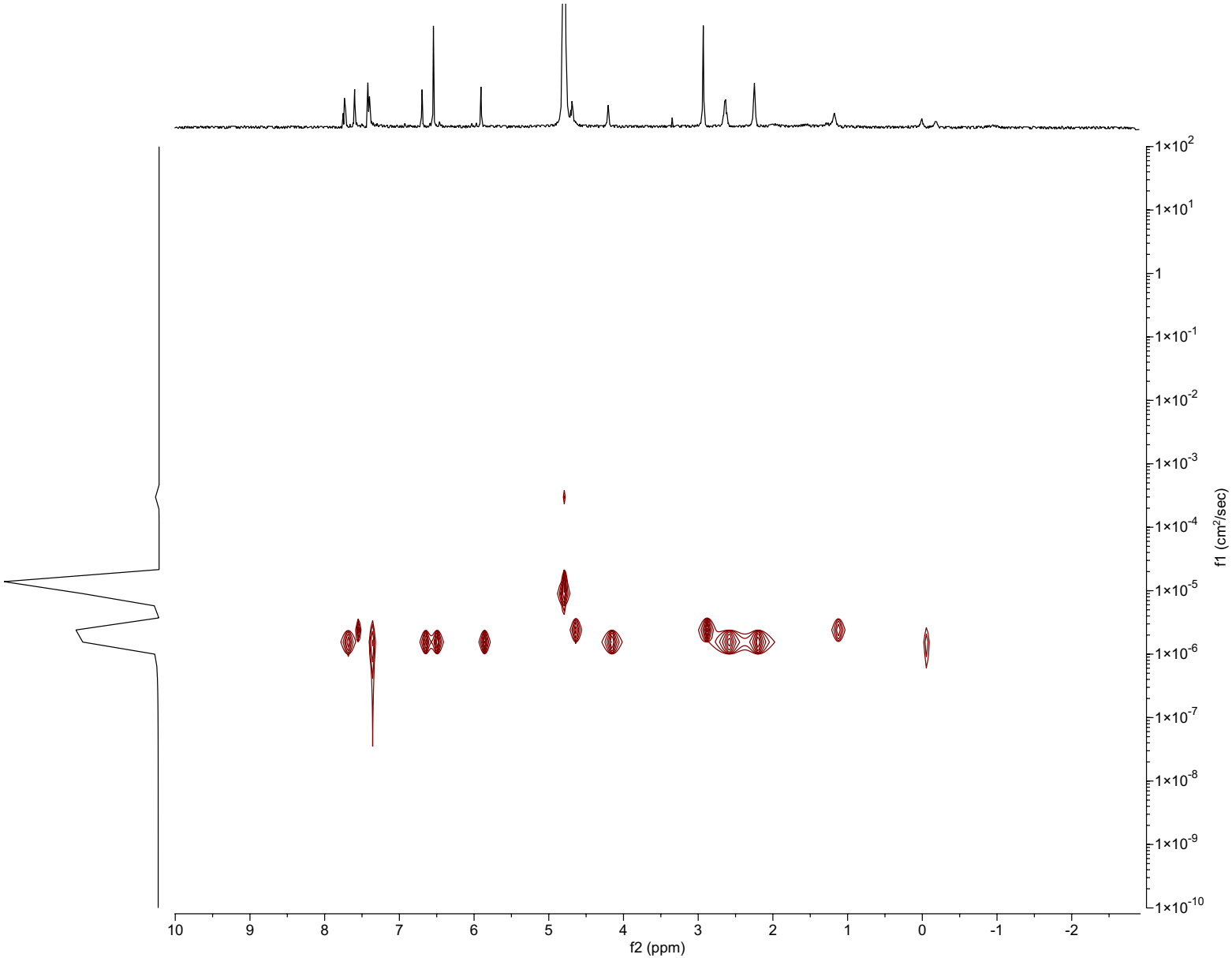

Figure S49: DOSY NMR spectrum of the 1:1 complex of ***exo*-OA** and **G8**. $D \approx 1.8 \times 10^{-6}$ cm^2 s^{-1} corresponding to a monomeric (non-capsular) complex.

I. Simulation Studies

We performed molecular dynamics (MD) simulations to understand the roles of cavitand host structure on their interactions with non-polar guests. Simulations were performed in the isothermal-isobaric ensemble at 25˚C and 1 atmosphere using GROMACS 2016.3.[15] The temperature and pressure were controlled using the Nosé−Hoover thermostat[16, 17] and Parrinello−Rahman barostat,[18] respectively. The cavitands simulated were OA and *exo*-OA, as well as a third (theoretical) host referred to as tri-*exo*-mono-*endo*-OA (TEMEAO), which differs from *exo*-OA by repositioning one of the rim carboxylates from an *exo* position to a neighboring *endo* position. The guest simulated was adamantane, which serves as a model hydrophobic guest moiety. The hosts, guest, and counterions were modelled using the Generalized Amber Force Field (GAFF)[19] with partial charges assigned from AM1-BCC calculations.[20] The net charge of each cavitand was set to −8e, obtained by deprotonating all host acid coating groups at the foot and rim of the host. Eight sodium cations per host were included to neutralize the host charge. Water was modeled using the TIP44P/Ew potential. Lennard-Jones interactions between unlike groups were obtained using Lorentz-Berthelot combining rules.[21] Non-bonded Lennard-Jones interactions were truncated beyond a separation of 9 Å, with a mean field dispersion correction for longer-range contributions to the energy and pressure. Electrostatic interactions were evaluated using the particle mesh Ewald Summation method with a real space cutoff of 9 Å.[22] Bonds involving hydrogens for the hosts and guests were constrained using the LINCS algorithm,[23] while water was held rigid using SETTLE.[24] The equations of motion were integrated using a time step of 2 fs.

Three types of simulations were performed. In the first set of simulations we considered a single host (OA, *exo*-OA, or TEMEOA) in a bath of 2000 water molecules to examine the hydration of the individual host pockets. These simulations were conducted for 100 ns following at least 5 ns for equilibration.

In the second set of simulations performed, we examined the hydrogen bonding between the host carboxylates between a single host (OA or *exo*-OA) and solvating water molecules upon the binding of an adamantane guest. In these simulations, the host-guest pair was solvated in a bath of 5000 water molecules. To align the cavitand along the *z*-axis of the simulation box, restraint potentials were applied to two dummy atoms along the C_4-axis of each host. The first "bottom" dummy atom was determined by the average position of the atoms connecting the four charged pendent groups of the cavitand to the bottom row of aromatic rings, while the second "top" dummy atom was determined by the average positions of the four carbon atoms on the second row of the aromatic rings closest to the cavitand portal. The dummy atom at the bottom of the binding pocket was spatially restrained with a harmonic force constant of 100,000 kJ/ (mol nm^2), while the vector connecting the bottom atom to the top was fixed along the z-axis using a harmonic angular constraint of 50,000 kJ/mol. The guest center was restrained to the C_4-axis of the host using a harmonic potential acting normal to the symmetry axis with a force constant of 100,000 kJ/(mol nm^2). The center of the guest was taken as the center of mass of the guest. Sampling windows were simulated from 5 Å deep-inside the cavitand pocket, measured from the center of the top plane defined by the four carbon atoms on the second row of aromatic rings closest to the cavitand mouth, to 15 Å out into the bulk solvent. Forty overlapping windows were used along the *z*-axis of box with the harmonic umbrella potential minima separated in 0.5 Å increments and a force constant of 15,000 kJ/(mol nm^2). Each simulation window was equilibrated for 1 ns, followed by a 15 ns production run. For each of these windows, hydrogen bonds were defined as $O_h \cdots O_w$ distances of < 3.2 Å, and a bond angle of ≤ 30˚.

In a third set of simulations, we evaluated the potential-of-mean force (PMF) between a single host (OA or *exo*-OA) and guests **G3** and **G4**. The PMF represents the relative free energy

of the system as a function of the distance between the host and guest positions. As such, the PMF provides a measure of the affinity of the guest to sit in the host pocket. The PMFs were determined using umbrella sampling.[25] During these simulations, the hosts were restrained to a single orientation as described above. The guest centers-of-mass were restrained along the *C4*-axis of symmetry of the hosts using using a harmonic potential acting normal to the symmetry axis with a force constant of 100000 kJ/(mol nm^2). The guests were allowed to move along the *C4*-axis (*z*) over a series of harmonic windows allowing the guest to sample portions of the PMF. Forty overlapping windows were used along the *z*-axis with the harmonic umbrella potential minimum separated in 0.5 Å increments and a force constant of 15000 kJ/(mol nm^2). Each simulation window was equilibrated for 1 ns, followed by a 15 ns production run. System configurations were saved every 0.2 ps for post-simulation analysis. The PMF was reconstructed from the overlapping windows using the weighted histogram analysis method. [26] The results of the PMF analysis are reported below in the supporting information.

Potential-of-mean force between hosts OA and exo-OA and guests G3 and G4. Figure S50 shows the PMFs between hosts **OA** and ***exo*-OA** with guests **G3** (Fig. S50a) and **G4** (Fig. S50b). In all cases the PMFs exhibit a deep minimum corresponding to the guests bound within the host pockets. The minima for **G4** is shifted to the right of that of **G3** as a result of **G4** being longer than **G3**. Both guests exhibit a preference for **OA** over ***exo*-OA** as indicated by the deeper PMFs for both guests with **OA** over ***exo*-OA**. As indicated by the difference in PMF minima, **G3** prefers **OA** over ***exo*-OA** by –15.1 ± 0.7 kJ/mol (= –77.5 kJ/mol – –62.3 kJ/mol), while **G4** prefers **OA** over ***exo*-OA** by -8.6±0.8 kJ/mol (= –60.7 kJ/mol – –52.2 kJ/mol). These free energy differences reflect the great affinity of both guests for OA and Exo-OA as reported in Table 1. While the PMF minima does not correspond to the binding free energies determined from ITC, it is heartening to note that the free energy differences determined from ITC (–19.8 kJ/mol for **G3** and -13.2 kJ/mol for **G4**). These differences reflect the influence of both Coulombic repulsion between the anionic moieties of the guest and the carboxylates of ***exo*-OA** as well as the drying and hydrogen-bonding contributions discussed in the paper.

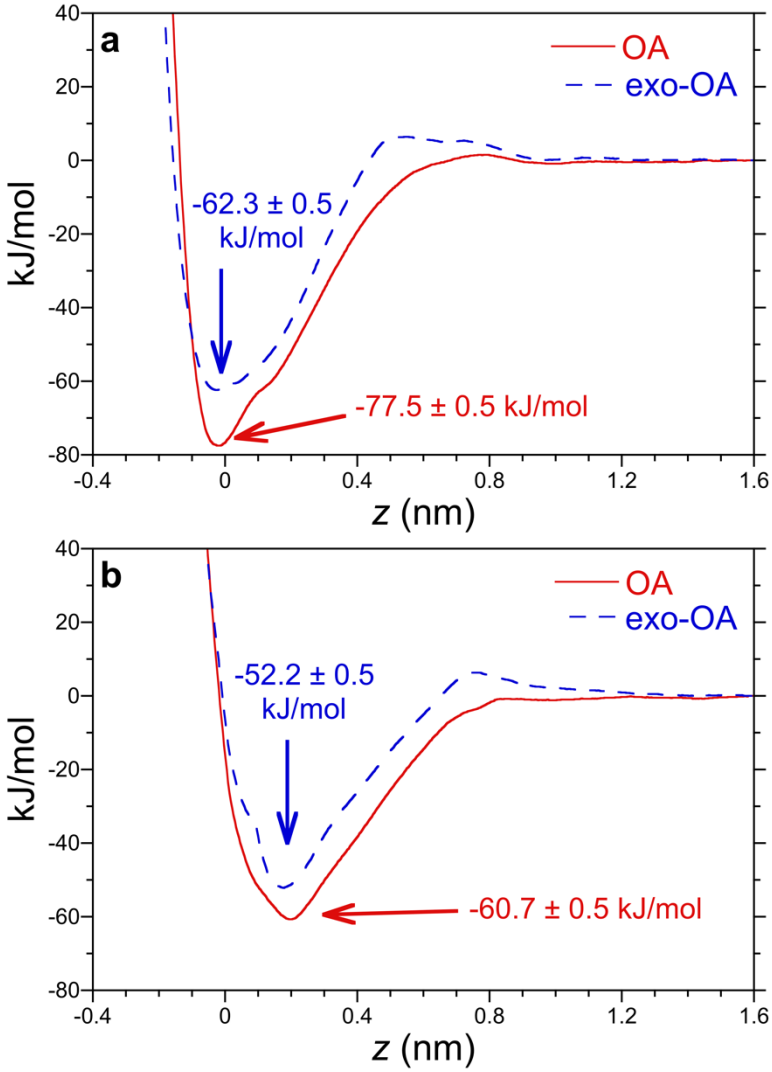

Figure S50: Potentials-of-mean force between hosts **OA** and ***exo*-OA** and guests **G3** (**a**) and **G4** (**b**) along the *C4*-axis of symmetry of the hosts (*z*) as determined from simulation. The figure lines are defined in the legend. The PMF minima for each host-guest system are indicated by the arrows.

J. References

1. H. Kakwere, R. J. Payne, K. A. Jolliffe and S. Perrier, *Soft Matter*, 2011, **7**.
2. H. O. House, C.-Y. Chu, J. M. Wilkins and M. J. Umen, *J. Org. Chem.*, 1975, **40**, 1460-1469.
3. J. S. Buck, R. Baltzly and W. S. Ide, *J. Am. Chem. Soc.*, 1938, **60**, 1789-1792.
4. D. D. Tanner, R. Arhart and C. P. Meintzer, *Tetrahedron*, 1985, **41**, 4261-4277.
5. K. Ramalingam, M. Balasubramanian and V. Baliah, *Indian Journal of Chemistry*, 1972, **10**, 366-369.
6. K. M. Harmon and L. S. Nowos, *J. Mol. Struct.*, 1991, **249**, 141-147.
7. C. L. D. Gibb and B. C. Gibb, *J. Comput. Aided Mol. Des.*, 2014, **28**, 319-325.
8. M. R. Sullivan, P. Sokkalingam, T. Nguyen, J. P. Donahue and B. C. Gibb, *J. Comput. Aided Mol. Des.*, 2017, **31**, 21-28.
9. H. Sun, C. L. D. Gibb and B. C. Gibb, *Supramol. Chem.*, 2008, **20**, 141-147.
10. W. B. Turnbull and A. H. Daranas, *J. Am. Chem. Soc.*, 2003, **125**, 14859-14866.
11. J. Tellinghuisen, *Anal. Biochem.*, 2008, **373**, 395-397.
12. C. L. Gibb and B. C. Gibb, *J. Comput. Aided Mol. Des.*, 2014, **28**, 319-325.
13. D. Brynn Hibbert and P. Thordarson, *Chem. Commun. (Camb.)*, 2016, **52**, 12792-12805.
14. P. Thordarson, BindFit, www.supramolecular.org).
15. M. J. Abraham, T. Murtola, R. Schulz, S. Páll, J. C. Smith, B. Hess and E. Lindahl, *SoftwareX*, 2015, **1-2**, 19-25.
16. S. Nosé, *J. Chem. Phys.*, 1984, **81**, 511-519.
17. W. G. Hoover, *Phys. Rev. A*, 1985, **31**, 1695-1697.
18. M. Parrinello and A. Rahman, *J. Appl. Phys.*, 1981, **52**, 7182-7190.
19. J. M. Wang, R. M. Wolf, J. W. Caldwell, P. A. Kollman and D. A. Case, *J. Comput. Phys.*, 2004, **25**, 1157-1174.
20. A. Jakalian, D. B. Jack and C. I. Bayly, *J. Comput. Chem.*, 2002, **23**, 1623-1641.
21. M. P. Allen and D. J. Tildesley, *Computer Simulation of Liquids*, Oxford University Press, Oxford, 1987.
22. T. Darden, D. York and L. Pedersen, *J. Chem. Phys.*, 1993, **98**, 10089-10092.
23. B. Hess, H. Bekker, H. J. C. Berendsen and J. Fraaije, *J. Comput. Chem.*, 1997, **18**, 1463-1472.
24. S. Miyamoto and P. A. Kollman, *J. Comput. Chem.*, 1992, **13**, 952-962.
25. G. M. Torrie and J. P. Valleau, *J. Comput. Phys.*, 1977, **23**, 187-199.
26. S. Kumar, J. M. Rosenberg, D. Bouzida, R. H. Swendsen and P. A. Kollman, *J. Comput. Chem.*, 1992, **13**, 1011-1021.